

Lawrence Berkeley National Laboratory

Recent Work

Title

PERFORMANCE OF THE DAPR SYSTEM

Permalink

<https://escholarship.org/uc/item/8fp0p1h5>

Authors

White, Howard S.

Hall, Dennis.

Publication Date

1970-03-01

Submitted at the 10th International Conference
on Data Handling Systems in High Energy Physics,
Cambridge, England, March 23-25, 1970

UCRL-19723
Preprint

c. 2

RECEIVED
LAWRENCE
RADIATION LABORATORY

MAY 18 1970

LIBRARY AND
DOCUMENTS SECTION

PERFORMANCE OF THE DAPR SYSTEM

Howard S. White and Dennis Hall

March 1970

AEC Contract No. W-7405-eng-48

TWO-WEEK LOAN COPY

*This is a Library Circulating Copy
which may be borrowed for two weeks.
For a personal retention copy, call
Tech. Info. Division, Ext. 5545*

LAWRENCE RADIATION LABORATORY
UNIVERSITY of CALIFORNIA BERKELEY

3 W

UCRL-19723

DISCLAIMER

This document was prepared as an account of work sponsored by the United States Government. While this document is believed to contain correct information, neither the United States Government nor any agency thereof, nor the Regents of the University of California, nor any of their employees, makes any warranty, express or implied, or assumes any legal responsibility for the accuracy, completeness, or usefulness of any information, apparatus, product, or process disclosed, or represents that its use would not infringe privately owned rights. Reference herein to any specific commercial product, process, or service by its trade name, trademark, manufacturer, or otherwise, does not necessarily constitute or imply its endorsement, recommendation, or favoring by the United States Government or any agency thereof, or the Regents of the University of California. The views and opinions of authors expressed herein do not necessarily state or reflect those of the United States Government or any agency thereof or the Regents of the University of California.

PERFORMANCE OF THE DAPR SYSTEM

Howard S. White and Dennis Hall

Lawrence Radiation Laboratory
University of California
Berkeley, California

INTRODUCTION

The Digital Automatic Pattern Recognition (DAPR) System for the unassisted discovery and measurement of events in bubble chamber film has been described at previous conferences of this series¹⁻³). The objective of the DAPR process is to produce on magnetic tape a concise abstract of the usable information contained in each film image, and then, by means of a digital computer, to perform all further analysis procedures from the information stored on this data abstract tape.

The hardware for the DAPR system consists of a Flying Spot Digitizer (FSD) of the Hough-Powell type, attached to an IBM 7094-II computer. This hardware configuration has been used for physics measurements at Berkeley since 1963 as part of the HAZE system. HAZE performs automatic measurement of bubble chamber events under the guidance of manual scanning. DAPR makes use of this hardware without significant modification, and thus takes advantage of the reliability and precision which have been established during the measurement of nearly two million events in the HAZE mode of operation. A Tandem FSD which is now being fabricated to augment the measurement capacity will strongly resemble the original unit, differing only in those components most affected by the gains in laser and integrated circuit technology made since 1961 when the first FSD was designed.

Fundamental to the DAPR system is the process by which information on film is converted to a digital abstract on magnetic tape. Digitizings from the FSD are associated into track segments. Segments from the sweeps necessary to cover the image in both normal and orthogonal mode are then linked into tracks. Each track of each view is represented on the Data

Abstract Tape (DAT) by a set of average points uniformly distributed over the length of the track, and by a measure of bubble density in clear regions away from other tracks. This ionization information is contained in the counts of digitizings and the total intersections of the scanning spot with the track locus. Fiducials are recognized, and their measured locations are preserved. Other lines which are digitized at fixed locations in repeated views are deleted, along with tracklike point sets originating from marks exterior to the chamber image. What is preserved on the DAT is therefore a precision measurement of ionization and track locus with respect to reference fiducials, exactly corresponding to the measurements made by HAZE, except that every track in every abstracted image is so recorded.

In order that the scanning programs which make use of the DAT can readily perceive events, further information describing the association of tracks is stored on the tape at the time of image abstraction. Verticies are detected in each view as being the clustering of track ends, confirmed by the determination that all associated tracks intersect at a common point. Coincidences due to viewing point are resolved by interview comparison. Final association of tracks in each view with a spatial vertex is made for tracks which can be matched in space. A table which summarizes this association of tracks and verticies in the three views is contained on the DAT, in addition to the track measurements.

Generation of the DAT is performed at a rate established by the FSD measurement speed. Film of small chambers, such as the LRL 25" HBC, requires about two seconds per normal or orthogonal view measurement, so that when stage retrace and film motion is included, an elapsed time of about 24 seconds is required to measure the three views on one bubble chamber exposure. Thus the one FSD unit yields a measurement rate of about 150 triads abstracted per hour. The central processor of the IBM 7094-II computer is occupied somewhat less than half time in controlling the FSD and achieving the data abstraction. A second or tandem FSD unit is expected to increase the measurement rate by about 1.8. Part of the computer capacity will remain available for background computations even when both FSD units are active.

The DAPR scanning process operates without further reference to the bubble chamber film. Events are selected by applying scanning criteria to the

detected vertices listed on the DAT, and the track measurements are edited into the HAZE library format for subsequent processing through geometry and kinematics programs. Because the vertices are stored on the DAT in a form readily perceived by the digital scanning process, comparison of scanning criteria with measured data to recognize desired events proceeds at a very rapid rate. Depending upon the number of events to be written out to the HAZE library tape, the rate of scanning is from 12,000 to 15,000 triads per hour.

COMPARISON EXPERIMENT

The best determination of the performance of a new system is obtained by comparison of its results for a substantial number of events with those obtained from some other well understood system. Film from a 1.53 GeV/c π^+ exposure of the LRL 25" Hydrogen Bubble Chamber was chosen for this comparison. This film had recently been analyzed for 2-prong events by use of the HAZE system, and for 4-prong events by use of the COBWEB system of online Franckensteins⁴⁾, so that a three-way comparison seemed possible. Furthermore, the LRL 25" HBC is optically clean, having two glass sides which allow images uncluttered by side effects of the illumination. The low momentum pion beam produces simple event types with a minimum of scanning ambiguities. And finally, there remains a sizable quantity of unmeasured film of this type and momentum region. However, the film chosen was not as good as we might have wished. In particular, the beam tracks are too closely spaced for best results. It was also discovered in the course of the DAPR measurement that static electric discharges in the camera produced images which caused serious problems for positioning views on the FSD. These positioning errors also lowered the completion ratio of the HAZE measurement.

COMPARISON PROCEDURE

Eight contiguous rolls were selected for comparison. All 13,005 frames were processed to form a DAT. Although prescanning in the form of HAZE roads existed, we chose to operate DAPR in the entirely unassisted mode. Only after the scanning program had selected vertices for assignment was it made aware of the HAZE scanning information, so that appropriate error codes could be assigned for bookkeeping purposes to unselected vertices which had been found by the HAZE scan.

Because comparison of the measurements on a track-by-track basis was desired, it was necessary to ensure that the track labeling be done in the same manner for both DAPR and HAZE measurements. The HAZE labels initially had been assigned by the scanners, and experience has shown that some inconsistencies of labeling are characteristically present. Therefore, the HAZE measurements were converted to the format of the DAT, and the tracks were relabeled by the DAPR scanning process. This procedure guaranteed identical labeling while causing only minute differences to the event throughput; we observed 84.6% throughput for the 2-prong events as a direct result of the HAZE measurement, and 84.4% throughput for the same data with the DAPR relabeling. It is of interest to compare these values with the normal throughput value of 92% for what is considered typically good film, giving evidence that the film selected for the comparison was below the usual quality.

The chamber volume in which vertices were accepted was limited for both the DAPR and HAZE scans. For DAPR, the limit at the entrance side of the chamber was set by the requirement in the scanning criteria that the incident track be measured over a sufficient length to establish that it was a beam track, while the limit at the exit side was set only by the need for outgoing tracks to be unambiguously matched. On the other hand, the HAZE scanners were instructed to accept events in which the incident track, even though short, appeared to follow the orbit of a beam track, allowing a much earlier acceptance region than for DAPR. Similarly, the HAZE criteria at the exit side took into account the requirement for kinematical uniqueness, and forced the acceptance volume to be more restricted than would have been required for track matching alone. The intersection of these two volumes, which is illustrated in Figure 1, will be referred to as the "joint fiducial volume" (JFV).

There are only 462 4-prong events within the joint fiducial volume. These yielded results similar to those derived from the comparison of the 2-prong events between DAPR and HAZE. On the other hand, the small number of events and the different basis of comparison (COBWEB rather than HAZE), makes the 4-prong data difficult to quantitatively relate to the larger data set. Therefore, we shall restrict the detailed discussion to the 2-prong data.

A simple set of scanning criteria was formulated to identify the 2- and 4-prong events to the DAPR scanning program. These criteria were intentionally conservative, so that any residual track match or vertex association ambiguity would cause the vertex to remain unselected as a desired event. The scanning criteria imposed the following requirements: The measured parameters for the incident track were required to be consistent with the defined beam orbit. Charge conservation was imposed. The vertex was required to have at least one track associated with it in each view. At least two view measurements with suitable geometry for reconstruction were required for each track.

COMPARISON RESULTS: THROUGHPUT

One basis for comparison of measurements is the number of events which are available to the kinematics programs. Of interest is not only the ratio of geometry completions to total events, but so also is the nature of the events which fail to be satisfactorily measured.

A total of 3140 2-prong events was found within the joint fiducial volume in the 13,005 frame sample of film. This total includes 2957 events found by the HAZE scanner, as well as 183 events newly found by DAPR. After a very painstaking scan of part of the film, we believe that it is unlikely that more than 2% of the total 2-prong beam event sample is not counted within this total number.

The distribution of these events according to whether their measurements passed or failed geometry is shown in Figure 2. Somewhat more than half of the events (1752 = 55.8%) had both HAZE and DAPR measurements pass satisfactorily through the geometric reconstruction. These events will form the basis for a detailed comparison of track parameters to be discussed below. The remaining 1388 events had no geometric output from one of the HAZE or DAPR sources, or both. Note that in the case of HAZE measurements, most of these events were found by the HAZE scanner, but had their measurement rejected for some reason. In like manner, most vertices were found by the DAPR process, but the track measurements were such that the DAPR event selection criteria were not met. This distribution therefore addresses the throughput efficiency, not the finding efficiency. These categories will be discussed in more detail in the following sections.

DAPR RESULTS MISSING

Results from geometric reconstruction are not present for the DAPR measurements described in Figure 2 under the categories "HAZE ONLY" and "NEITHER". The 722 events (23.0%) included in the "HAZE ONLY" category are those found by the HAZE scanner, and satisfactorily measured by HAZE, but either undetected or unselected by DAPR. The 252 events (8.0%) marked "NEITHER" include 17 which were unseen by the HAZE scanner, but were selected by the DAPR scanning program and then failed in the geometric reconstruction. The 974 events in these categories were inspected at the scanning table, and each event was classified according to the apparent cause of its failure. This classification was based upon the coded comment supplied by DAPR and upon the appearance of the event and its surroundings as viewed at the scanning table. Figure 3 shows the distribution of these assigned causes.

Film format problems which prevented one or more views from being properly positioned by the FSD caused the rejection at abstraction time of frames containing 5.0% of the JFV sample. Nearly all of these are due to static discharges made in the camera which introduced confusion in the area of the edge markings by which the view is positioned. This is not a common problem in 25" HBC film, and undoubtedly contributed to the lower HAZE throughput observed for this film. If we correct the throughput ratio for these events, we obtain a DAPR throughput of 72.6%, which indeed was exceeded for the first six of the eight rolls.

Many of the events which could not be selected were victims of their surroundings. These are shown in the next major division of Figure 3. Although the events are well distributed across the chamber in the total sample, the tracks of any one beam pulse are rather tightly clustered. The most significant result of such overlaid beam tracks was the addition of a track or tracks which could not be excluded from the vertex, which therefore produced geometric ambiguities that prevented the clear choice necessary for event selection. This class is indicated as "Close Beam Tracks" in the distribution. An example of such an event is shown in Figure 4, where the forward outgoing track was confused with the nearby beam track enough to produce a poor vertex point, thereby excluding the backward track.

In some cases, two events were sufficiently close to confuse the vertex generating algorithms of DAPR. This caused all of the tracks of both vertices to be gathered into a single vertex producing the logical "OR" of the tracks. The class is so named.

Some events are made ambiguous by the presence of an unrelated, but spatially coincident track which ends nearby. We call these tracks "interlopers", and the class is named accordingly. An example of this is shown in Figure 5, where a track produced at a vertex near the entrance ends quite near a 2-prong event in the lower half of the picture.

The following of an electron spiral of a few centimeters radius is generally quite incomplete, giving rise to several short segments which represent part of the total spiral. When one of these passes through a vertex, it usually produces an ambiguity which the program cannot presently resolve. An example of this "Electron Spiral" class is shown in Figure 6.

For a considerable fraction of the DAPR measurements not output through geometry, there is an apparent dependence upon configuration. These are shown in another major division of Figure 3. Most of these configuration dependent selection failures are in the category of "Vertex Algorithm" failures. The only algorithm presently incorporated in the DAPR vertex search routine depends upon the presence of two or more track endpoints near each other, with at least one endpoint being quite near the intersection point of the two tracks. One large subset of 2-prong events is guaranteed to fail this search algorithm: those events in which one outgoing track departs from the vertex in a direction essentially parallel to the incident track. Small angle elastic scatters and inelastic events are both observed in the "Vertex Algorithm" failure category. The present algorithm is by no means the only one feasible, and it soon will be augmented by another algorithm especially tailored to pick up these events. An example of "Vertex Algorithm" failure is shown in Figure 7, where the elastic scattering produced by the beam track nearest the right side of the picture is followed as a continuation of the incident track. In Figure 8, the inelastic event is most obvious as a change of bubble density fairly early in the chamber, and no significant deviation of the beam track is seen for some distance. The presence of a number of close beam tracks makes this picture difficult for visual inspection as well.

The DAPR program is conditioned to retain only tracks on which a minimum of twelve hits have been made. This minimum requires that the track be at least 720 microns in projected length along the direction of the stage travel. Tracks in the bubble chamber shorter than 1.5 centimeters generally are not found by DAPR because of this requirement, giving rise to the selection failure class "Short Stub". An example of this is shown in Figure 9, where the shorter of the two elastic recoil tracks is approximately at the limit of being seen by DAPR track following.

A short track outgoing from a primary event which leads to a nearby secondary event is similar to the category of "Vertex OR" previously discussed, except that of course this class is produced by the event configuration. An example of "Short Secondary" is shown in Figure 10, where the left-most beam track produces a 2-prong event with a secondary 2-prong about 1 centimeter away.

Some event configurations have tracks obscured by other tracks of the event, as in the 4-prong event shown in Figure 11. Others have tracks so placed that the three-view geometric reconstruction cannot produce a unique match of the track-views, as is illustrated in Figure 12 by the 2-prong event with coincident tracks at the bottom of the picture. These classes are indicated in Figure 3 by the legends "Configuration Precludes Track Following" and "Ambiguous Tracks".

A few of the events detected by the DAPR vertex search, and selected by the DAPR scanner, failed the three-view geometry program FOG. However, for a number of events, no apparent reason for failure was seen when they were viewed at the scanning table; these were assigned to the category "Reason Unclear". They have since been studied in detail by use of various diagnostic procedures. Some are found to result from frame positioning errors undetected by DAPR, errors which caused one view of some other triad to be measured in place of the correct one. Some events have tracks which extend beyond the usual region of chamber illumination, so that the track was rejected as unwanted noise. The latter can be corrected merely by changing a constant within the program. The event in Figure 13 that is produced by the right-most beam track contains such a track, extending out beyond the chamber image to the left of the picture.

Not all of the events which remained unselected by the DAPR scanning program failed to have a detected vertex. Figure 14 shows the distribution of undetected vertices among the 974 events not output by DAPR which have just been discussed. It should be noted that correction of the causes yielding "Film Format" and "Vertex Algorithm" failures will reduce to only 3% the fraction of vertices unperceived by DAPR, with half of these due to close beam tracks. This compares, as we shall see, to nearly twice this number of events missed by the HAZE scanner.

DAPR EVENTS NOT OUTPUT BY HAZE

Each event output by the geometry program from the DAPR measurement, but not from the HAZE measurement was carefully reviewed at the scanning table. The 414 valid 2-prong events are distributed between those which were found, and those which were missed by the HAZE scanner in the manner shown in Figure 15. Allowance has been made to credit the HAZE scanner with finding the event when procedural or scanning hardware errors prevented the HAZE measurement from being successful. Even so, 166 events, or 5.3% of the total sample were not detected by the manual scanning process. There were no obvious features to distinguish any of these events from the total distribution, except that the HAZE scanner missed events invisible in the one view which he scanned.

An additional 43 vertices from the 13,005 frame JFV sample successfully met the criteria which were given to the DAPR scanning program, but proved upon inspection not to be valid 2-prong events. The distribution of these 43 "fake" events as determined by scanning table inspection is shown in Figure 16.

The eight secondary events were selected by the DAPR scanner only because of an oversight in writing the scanning criteria, which neglected to require that "beam events" must have an incident track that actually enters the chamber.

The classes of "Short Sigma" and "Short Secondary" are due to DAPR's inability to see short tracks. Their frequency can be reduced by tightening the tolerance by which tracks are allowed to miss the common intersection point. Some of the 4-prong events have one very faint track, which digitizes so poorly that it is not followed. If this track is caused by the negative

particle, and if the forward positive sufficiently resembles a beam track, the track match routines delete the "outgoing beam" track, leaving an apparently valid 2-prong event. This happened in nine cases. On the other hand, the deletion of an apparently "out-going beam" track allowed the selection of perhaps 10% more 2-prong events which were very close to a neighboring beam track. Finally, some adjacent track endings meet all present criteria for both vertices and selected events.

We believe that the problem caused by these fakes is not serious. Many can be eliminated by small changes in the DAPR procedures and scanning criteria. Fakes which then survive will represent only a small increment to the set of fakes found by manual scanning, and can be guarded against in the kinematic analysis by the same means now used to eliminate scanning ambiguities and mistakes.

DAPR MEASUREMENT QUALITY

We now turn to the 1752 events for which geometry output (kinematic input) from both the HAZE and DAPR sources was available. In order to achieve a valid comparison of the two measurements, all tracks were fitted as pions in the geometry program FOG⁵⁾. This procedure was chosen since the orbital error introduced by fitting a proton track to a pion mass hypothesis is negligible, whereas fitting a pion track to a proton mass hypothesis produces serious discrepancies in the orbit at low values of momentum. Differences between the HAZE measurement and the DAPR measurement were computed for the dip angle, the azimuth angle, and the momentum at the vertex for each track. These differences were then normalized by dividing by the combined a priori error estimates for the two measurements. The difference between track length measurements was also computed but no normalization factor was applied. For all parameters the DAPR value was subtracted from the HAZE value so that a positive difference implies that the HAZE value was greater than the DAPR value and vice versa. Thus, for each track in the sample, comparison parameters were computed for the dip angle, the azimuth angle, the momentum, and the track length.

Qualitatively we would expect independent measurements of the same track to produce symmetric distributions centered at zero. Further, the standard deviation of these distributions should be somewhat smaller than

unity, since the normalization factors include a term which accounts for multiple scattering. Figure 20 shows the distribution of the normalized differences in dip angle summed over all three tracks. We notice that the observed distribution is entirely compatible with our a priori assumptions. Furthermore, there are very few tracks with large departures. The source of the few large departures has not been completely determined at the present time, although a number of these events have been studied. Improper vertex correlation by the event comparison program is certainly one source. Small angle scatters which were detected by the HAZE scanner, but not by DAPR have some contribution. There is some evidence that a priori errors may be underestimated for low momentum tracks. Whatever the source, these events are not believed to represent a serious contamination of the data, since their frequency is low.

Figure 21 shows the distribution of the normalized differences in azimuth angle summed over all three tracks. In this case we observe a somewhat wider distribution with a mean of -0.2 standard deviations. The increased width is probably due to a slight miscalculation in the error coefficient which was used for normalization, and does not reflect a basic error in either HAZE or DAPR. The shift in the mean represents an angular discrepancy of only $.016$ degrees on the average, or one minute of arc.

Figure 22 shows the distribution of normalized differences in momentum, and again, the two measurements are seen to be in excellent agreement. Thus the HAZE and DAPR systems are seen to be equivalent in their measurement of the three basic track descriptors.

In the case of track length, a somewhat more surprising result was obtained. We had assumed that the length of track measured by DAPR would be somewhat smaller than the length measured by HAZE on the average. In fact just the opposite was observed. Figure 23 shows the distribution of track length differences between HAZE and DAPR. Notice that this distribution is skewed even though it peaks at zero and has a standard deviation of about $.75$ centimeters in space. The number of events in which the HAZE measurement exceeded the DAPR measurement by more than 2 centimeters is negligible. However, there is a significant contribution of events in which the DAPR measurement was more than 2 centimeters longer than the corresponding HAZE measurement. A small fraction of these events are indeed due to kinks and

and other small angle departures detected by the HAZE scanner but not by DAPR. However the great majority of these events are due to the HAZE scanners ending the road prematurely. This unfortunate habit went unnoticed until the comparison experiment was performed. Since the ability to resolve kinematical ambiguities is strongly related to the length of track measurements, DAPR represents a significant improvement over our operating experience with a full guidance system.

A related question concerns what is the shortest track that can be measured by DAPR. Figure 24 shows the track length distribution for the proton track of elastic events. Tracks longer than 1.4 centimeters in space are seen to be consistently detected. This corresponds to 1 millimeter on film, or 17 hits if no angle projections are assumed. When a correction is applied for the average projection angle this value agrees exactly with the 12 hit cutoff in the DAPR track following process. A new procedure which accepts dense tracks with fewer hits is planned for the future.

Finally, Figure 25 shows the distribution of $\cos \theta^*$ in the center of mass system for the proton track of the elastic events ⁶⁾. The HAZE data was derived from the entire HAZE fiducial volume and normalized to the eight roll JFV sample. The normalized HAZE data is represented by the dotted line, and the DAPR data is represented by the solid line. The depletion of DAPR data in the first two cells, and in the last cell is due to the predicted bias from the as yet incomplete vertex algorithm and short stub procedures of DAPR. When the data in the central 37 cells were compared a χ^2 value of 8.0 was calculated for a 20 degree-of-freedom fit. Thus, except for predictable biases, the DAPR measurements are seen to be in excellent agreement with the HAZE measurements.

UNSELECTED VERTICIES

An investigation of all verticies detected by DAPR but not noted by the HAZE scanner was undertaken for one roll of the eight roll study. Obviously, not all event types in the film had been considered by the HAZE scanner; the distribution is presented here for two reasons. First, there is the practical consideration of how many frames per roll must be manually reviewed in order to be certain that no desired events were overlooked. Secondly, the distribution gives an indication of the DAPR finding efficiency for all event types

in the film. Unfortunately, no comparison data for event types other than beam 2- and 4-prong events was available. Thus finding efficiencies can not be reported for event types other than these. However, there is good indication that 2-prong events are the most difficult for DAPR to detect, and that the finding efficiency for other event types is excellent.

DAPR produced in the entire roll of 1663 frames a total of 108 verticies which were not recorded by the HAZE scanner. Figure 24 shows the distribution of these verticies by event type. Most (68) of these resulted from 2-prong events. Of these, 32 were valid beam events, with 20 selected by the DAPR scanner and 12 detected but unselected. In addition, there were 15 2-prong events produced by degraded beam particles, as well as 16 secondary scatters. The five fake events were among those already discussed.

The second largest category contains 22 events of all other types, consisting of 4 4-prong events, 5 events in the glass, 5 kinks, 5 electron pairs, 2 $\pi \mu \beta$ decays, and one V^0 from the chamber wall. The 5 events in the glass can be eliminated by applying a fiducial volume cut in the Z direction.

The final category consists of 12 verticies formed from unrelated tracks which happened to end near each other in space, together with 6 "verticies" which were not apparent when inspected at the scan table. Thus in 1663 frames, the DAPR procedure yielded only 18 verticies which were not the result of some sort of interaction.

The DAPR scanning program can be instructed to identify events of a given type without including them on the HAZE library tape for further analysis. Use of this procedure greatly reduces the number of frames which require manual review. Such identification is analogous to describing the signature of unwanted events in the manual scanning instructions so that they will not continually be brought to the attention of the experimenter. In this comparison experiment, for example, a description of the non-beam and secondary 2-prong events, and events in the glass would identify approximately 26 undesired events among the 108 verticies shown in Figure 24. The number of verticies remaining after selection or identification is therefore 57, or about 4% of the frames in the roll. Using these procedures, the DAPR scanning program can extract most desired events from the film

without manual assistance, and can produce a concise list of frames outside its scanning criteria for manual review.

PHYSICS PRODUCTION

The use of DAPR for physics measurements has now begun. The first film measured was from a 1.29 GeV/c π^+ exposure of the 25" HBC, which allowed the experience gained in the comparison experiment to be most directly applied. Because the bulk of the 2-prong events in this film had not previously been measured, manual scanning was used to provide a bookkeeping entry for each event found by the scanner. This prescan was most important in giving confidence to the experimenter that DAPR can indeed find his events adequately. However, since the events occur in about every third frame, by using the prescan information to select frames to be abstracted, the cost of the scanning is balanced by the saving in abstraction cost. The DAPR processing makes no use of the prescan information except for frame control. About 14,000 events were measured during the first week of operation in February, 1970. Prescanning has operated at a rate averaging 100 frames per hour or more. Measurement of frames selected has averaged 150 frames per hour with the DAPR system.

SUMMARY OF PRESENT STATUS

The comparison experiment provides a firm basis for confidence in the DAPR process as it now stands. We have shown that the tracks and vertices contained on the DAT are a high fidelity abstraction of the film information. Almost all events are perceived by DAPR. Nearly three-fourths are available to kinematic analysis without any manual assistance, and this fraction is increasing as gaps in program completeness are filled in. The list of vertices containing desired events that are perceived but unselectable contains but few extra entries. The measurement precision is equivalent to HAZE, our present standard of excellence. DAPR has now become a practical tool for high energy physics measurements.

Some parts of the system remain to be completed. Additional vertex algorithms are being implemented, as is the ability to follow shorter tracks. The art of writing scanning criteria has only begun to be explored. We hope that the impediments caused by format and close beam track difficulties will influence the design of future experiments.

DAPR is already superior to manual scanning systems in some ways. The full abstraction of all tracks allows calibration of ionization and of beam cross section on a frame-by-frame basis. Consistent adherence to desired standards can be more readily achieved with an automatic system than with a manual system employing many persons. The cost of discovering and measuring events is considerably reduced in comparison to HAZE and other systems.

THE FUTURE

We expect that DAPR can be operated with little change in chambers of the two-meter class, and steps to measure data from the SLAC 82" HBC are now being taken. Extension to the large scale chambers being designed will depend primarily upon the ability of the digitizing hardware to produce good representations of the information from the film. The procedures of DAPR, perhaps implemented on a larger computer, would seemingly perform as well for large chambers as small.

We believe that DAPR has already moved very close to the goal of totally unassisted analysis of bubble chamber data. Its achievement of this goal seems assured. With human reaction times no longer included in the system, it would be possible with suitable hardware to operate without film, online to the bubble chamber. This would allow for bubble chambers the same advantages of immediate, online data analysis which have been so useful in many spark chamber experiments, while retaining the precision and resolution of the bubble chamber. Only a system which operates without manual assistance can go online in this manner. We believe that the attainment of operational status by DAPR is a significant step toward these goals.

ACKNOWLEDGEMENTS

The development of the DAPR system has resulted from the efforts of many persons including several former members of the Data Handling Group who now have gone elsewhere. The hardware owes its fine design and performance to groups at IRL headed by Jack Franck and Gene Binnall. The continued interest, encouragement and firm support given to the project by IRL Director Edwin McMillan and Physics Division Leader David Judd have made it all possible.

This work has been supported by the U.S. Atomic Energy Commission.

REFERENCES

1. Howard S. White, et. al. "DAPR: Digital Pattern Recognition Approaches Production". UCRL-18542. Contained in the Proceedings of the International Conference on Advanced Data Processing for Bubble and Spark Chambers, Argonne National Laboratory, Argonne, Illinois, October, 1968.
2. Dennis Hall, "DAPR: Vertex Search and Track Match." UCRL-18544. ibid.
3. Joan Franz, "DAPR: Automatic Scan". UCRL-18546. ibid.
4. Herbert C. Albrecht, et.al. "The COBWEB Data Reduction System". UCRL-18528 Rev. ibid.
5. Shirley Buckman, et.al. "The Multi-View FOG Program and its Application to Quality Control of FSD Data". UCID-2652. Contained in the Proceedings of a Conference on Programming for Flying Spot Devices, Columbia University, New York City, N.Y. October, 1965.
6. George C. Kalmus, LRL (private communication).

FIGURE CAPTIONS

1. Joint Fiducial Volume for the Comparison Experiment.
2. Distribution of 3140 Two-prong Events within the Joint Fiducial Volume.
3. Distribution of 974 Events Not Output by DAPR.
4. Example of the class "Close Beam Tracks".
5. Example of the class "Interloper".
6. Example of the class "Electron Spiral".
7. Example of the class "Vertex Algorithm" (elastic event).
8. Example of the class "Vertex Algorithm" (inelastic event).
9. Example of the class "Short Stub".
10. Example of the class "Short Secondary".
11. Example of the class "Configuration Precludes Track Following".
12. Example of the class "Ambiguous Match".
13. Example of the class "Reason Unclear".
14. Distribution of 974 Events Not Output by DAPR showing Undetected Verticies.
15. Distribution of 414 Two-Prong Events Output by DAPR only.
16. Distribution of 43 Fake Two-Prong Events Found by DAPR in the Joint Fiducial Volume for 13,005 Frames Scanned.
17. Example of DAPR fake due to a forward track to the secondary vertex.
18. Example of a DAPR fake due to a short Σ decay.
19. Example of a DAPR fake due to a non-beam event coincident with a beam track.
20. Comparison of HAZE and DAPR measurements of Dip Angle.
21. Comparison of HAZE and DAPR measurements of Azimuth Angle.
22. Comparison of HAZE and DAPR measurements of Momentum.
23. Comparison of HAZE and DAPR measurements of Track Length.
24. Distribution of short Proton Recoil Lengths for Elastic Events.
25. Distribution of CMS Proton Recoil angle for Elastic Events.
26. Distribution of 108 Verticies Perceived by DAPR but Not Seen by the HAZE Scanner.

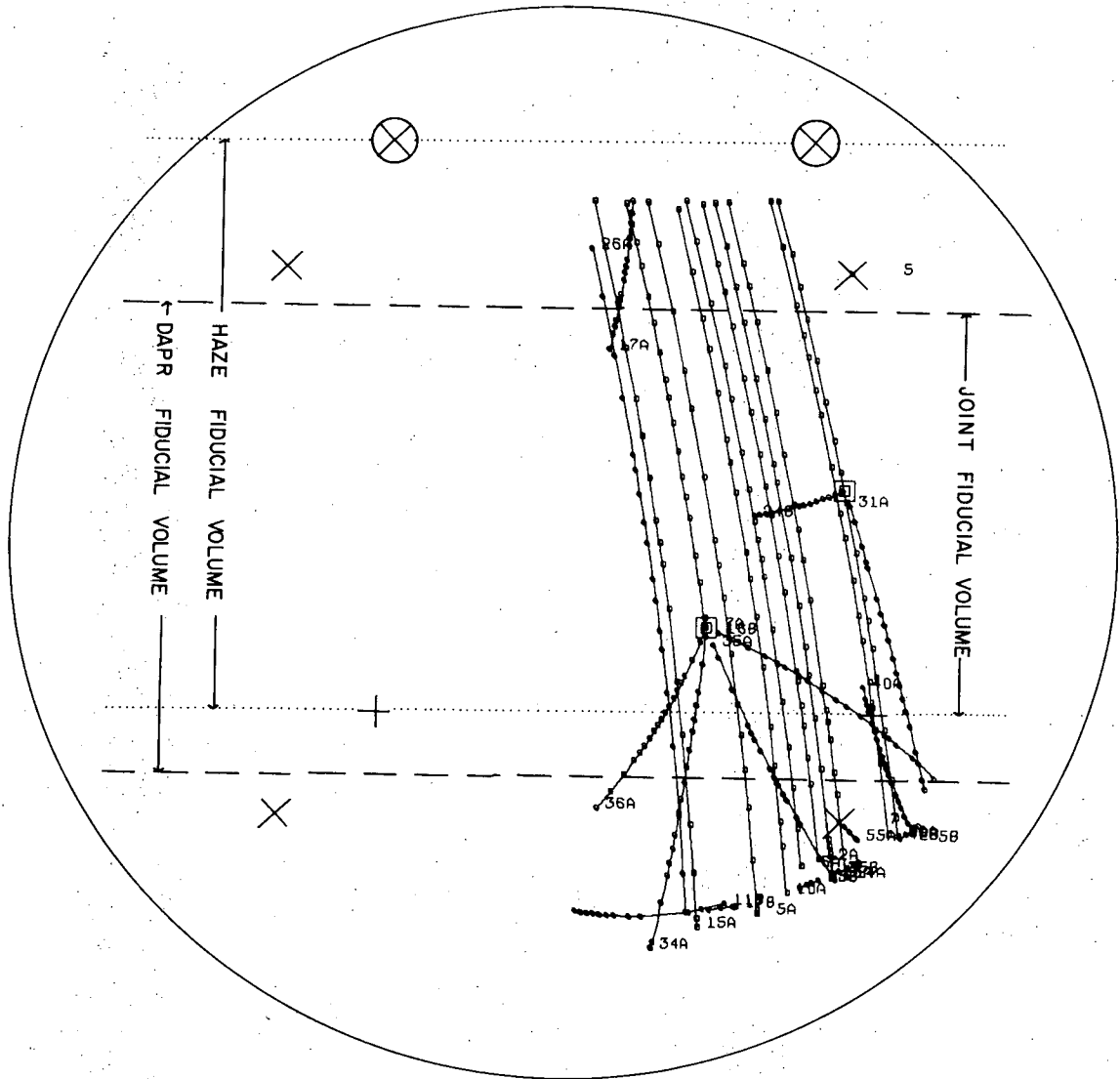
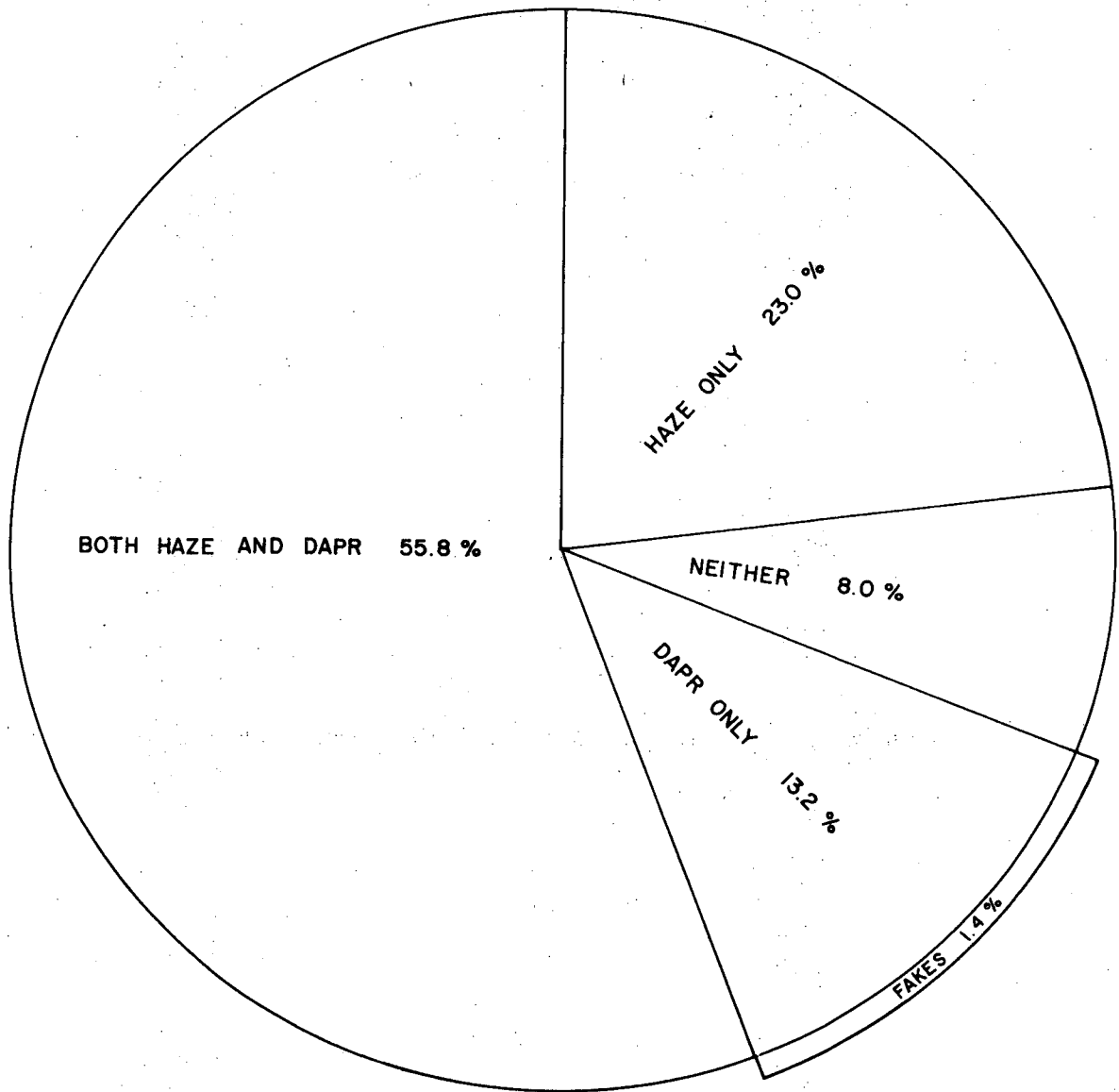


Fig. 1

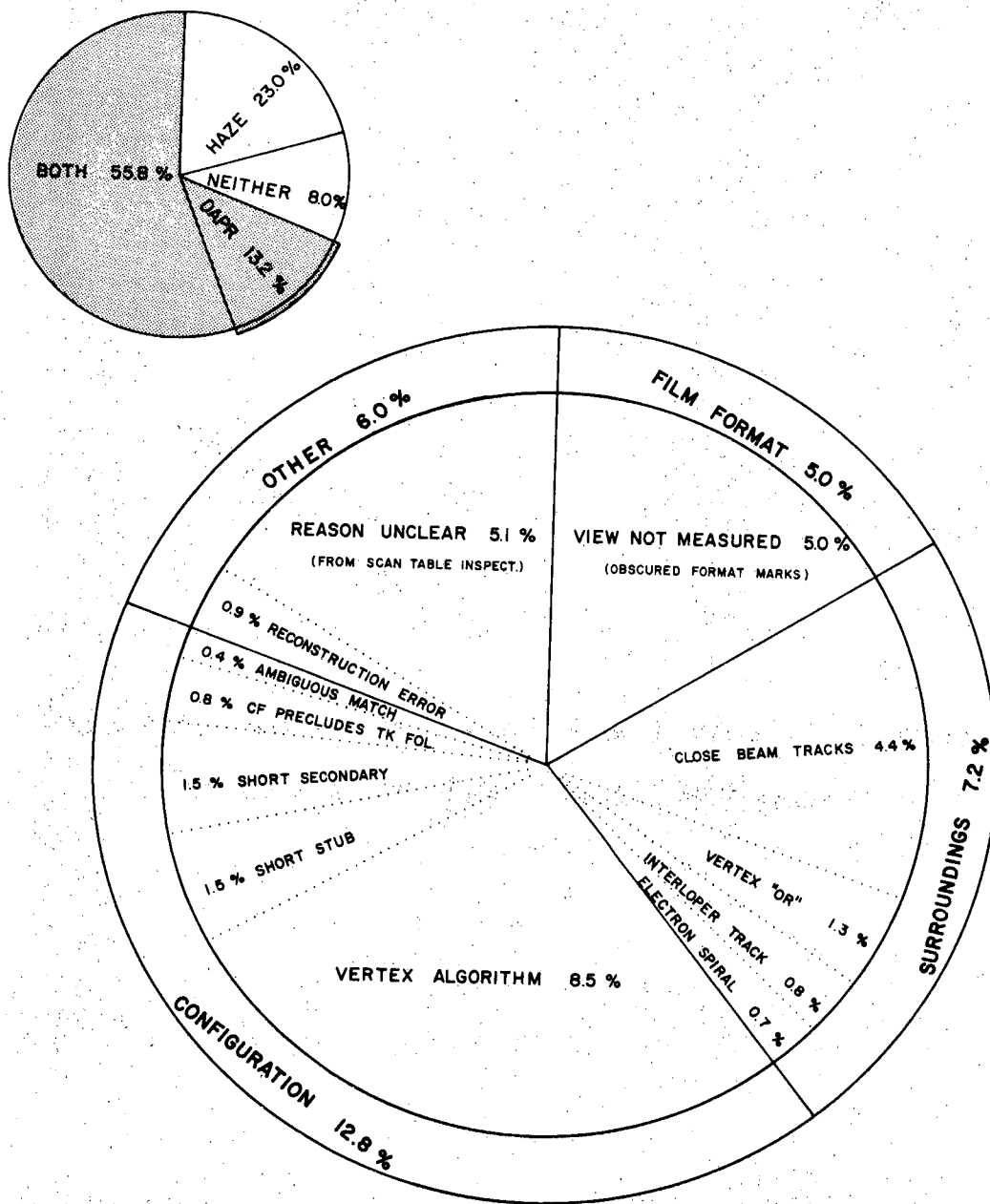
XBL 702-402



**DISTRIBUTION OF 3140 TWO-PRONG EVENTS
WITHIN JOINT FIDUCIAL VOLUME**

XBL 702-406

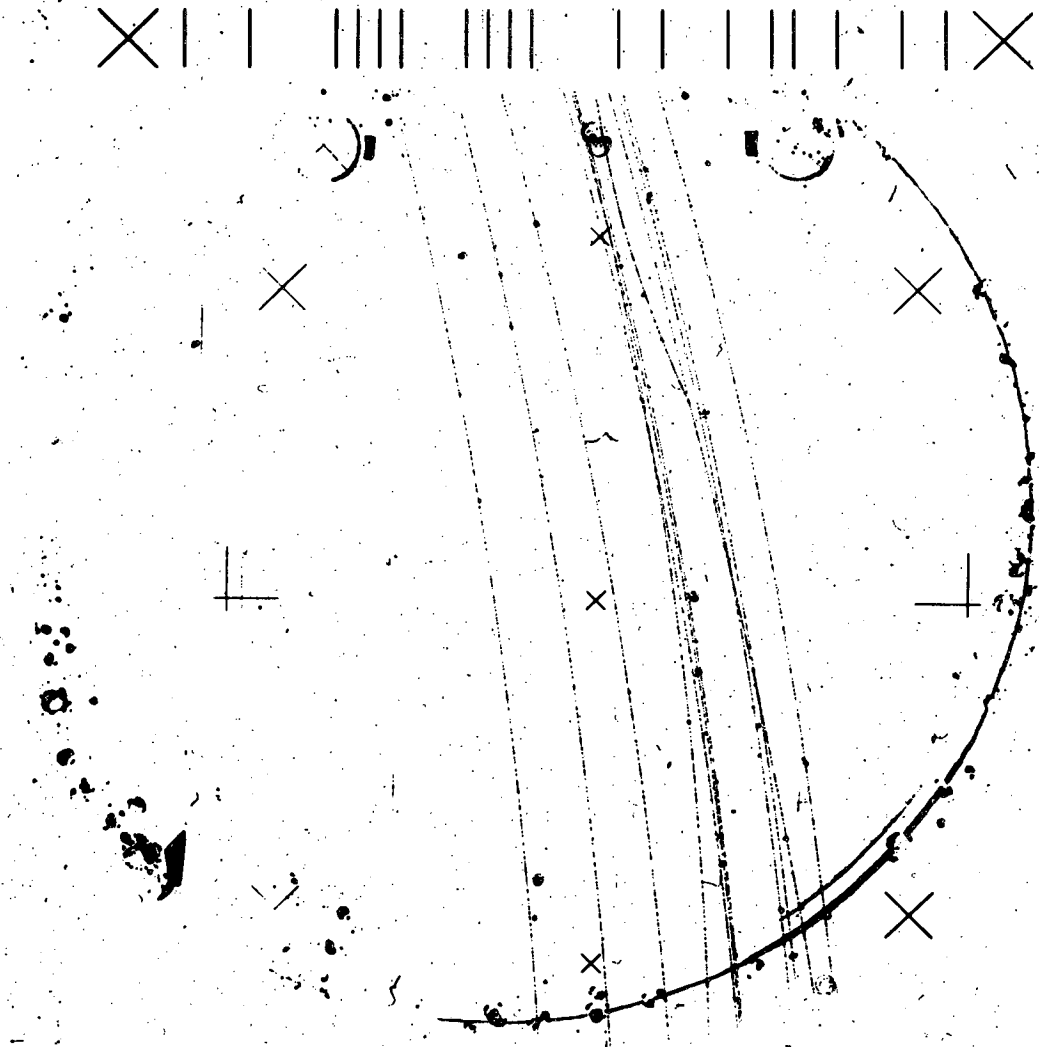
Fig. 2



DISTRIBUTION OF 974 EVENTS NOT OUTPUT BY DAPR
31.0 % OF 3140 EVENT JFV SAMPLE

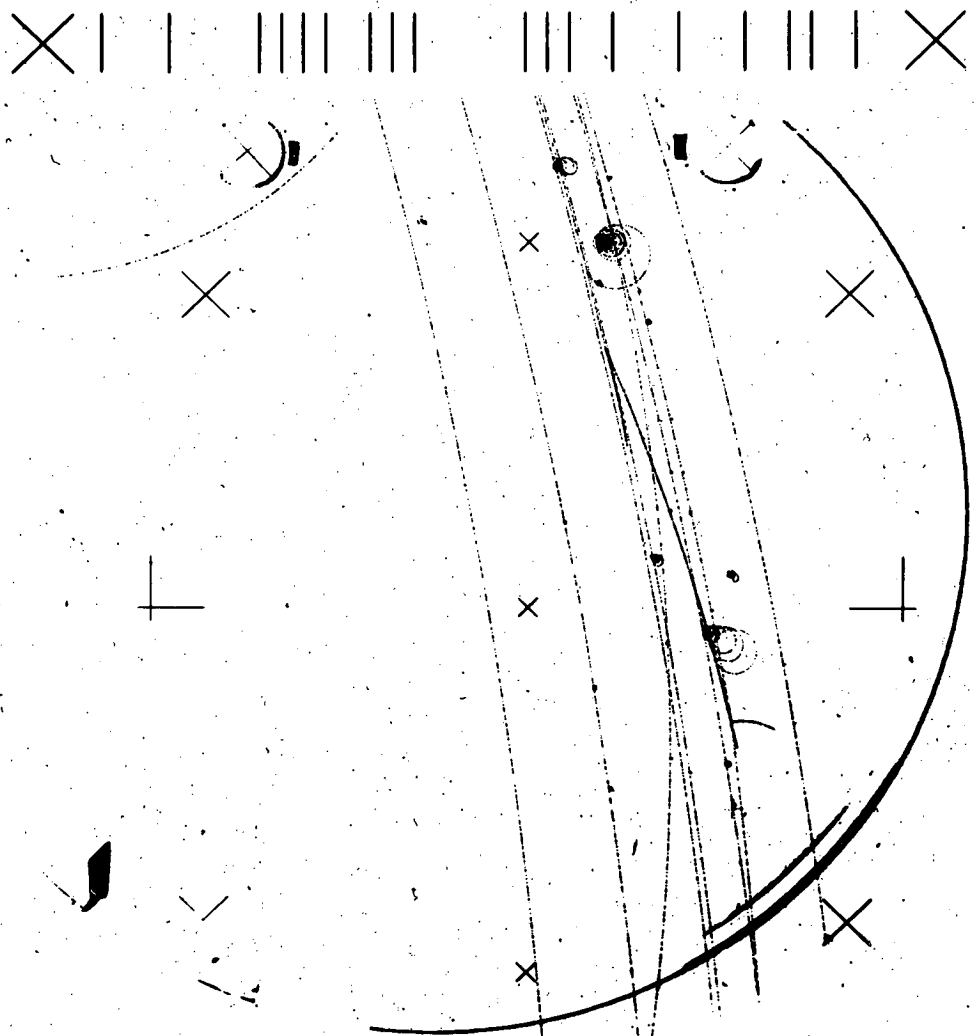
XBL 702-404

Fig. 3



XBB 702-904

Fig. 4



XBB 702-907

Fig. 5

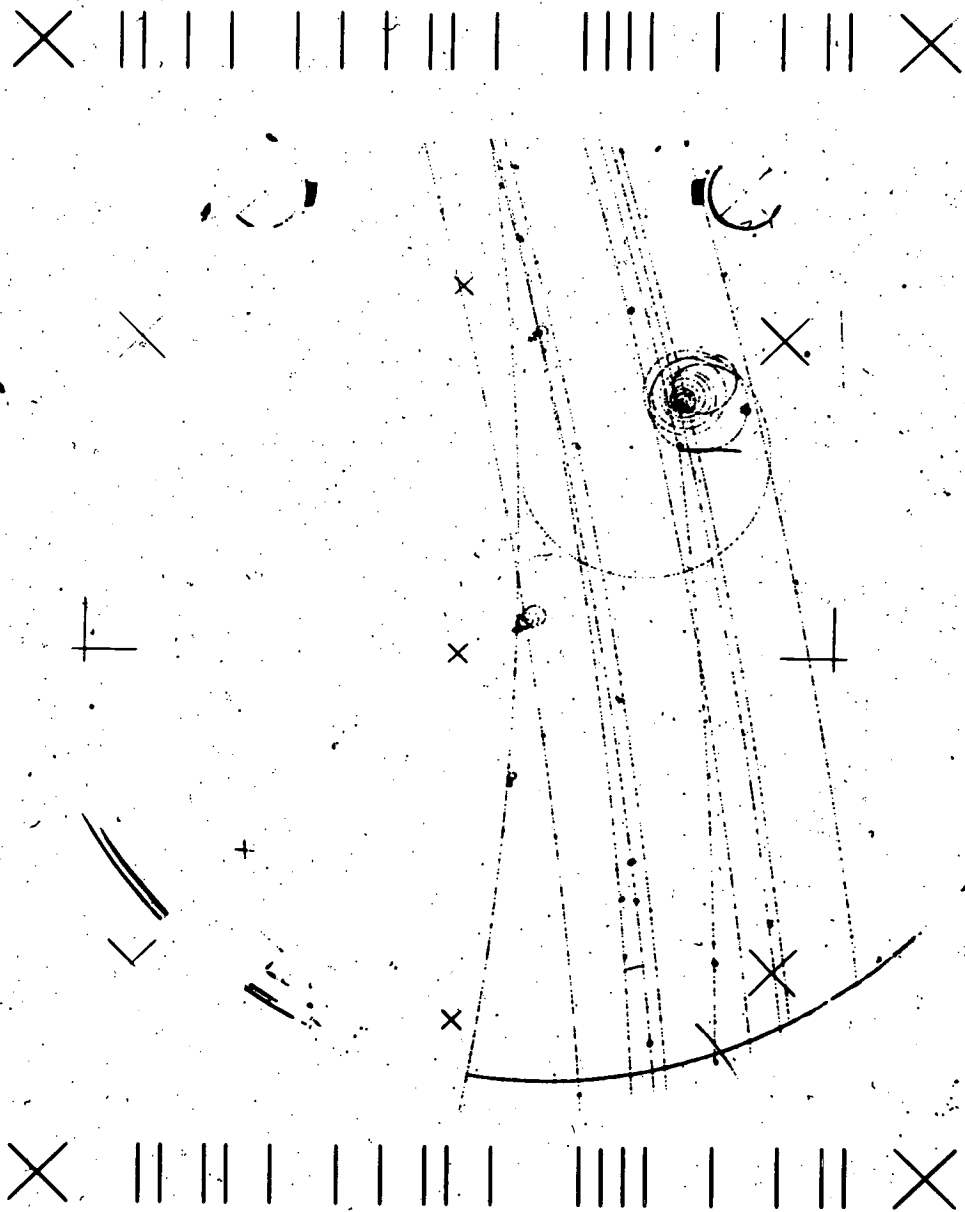


Fig. 6

XBB 702-911

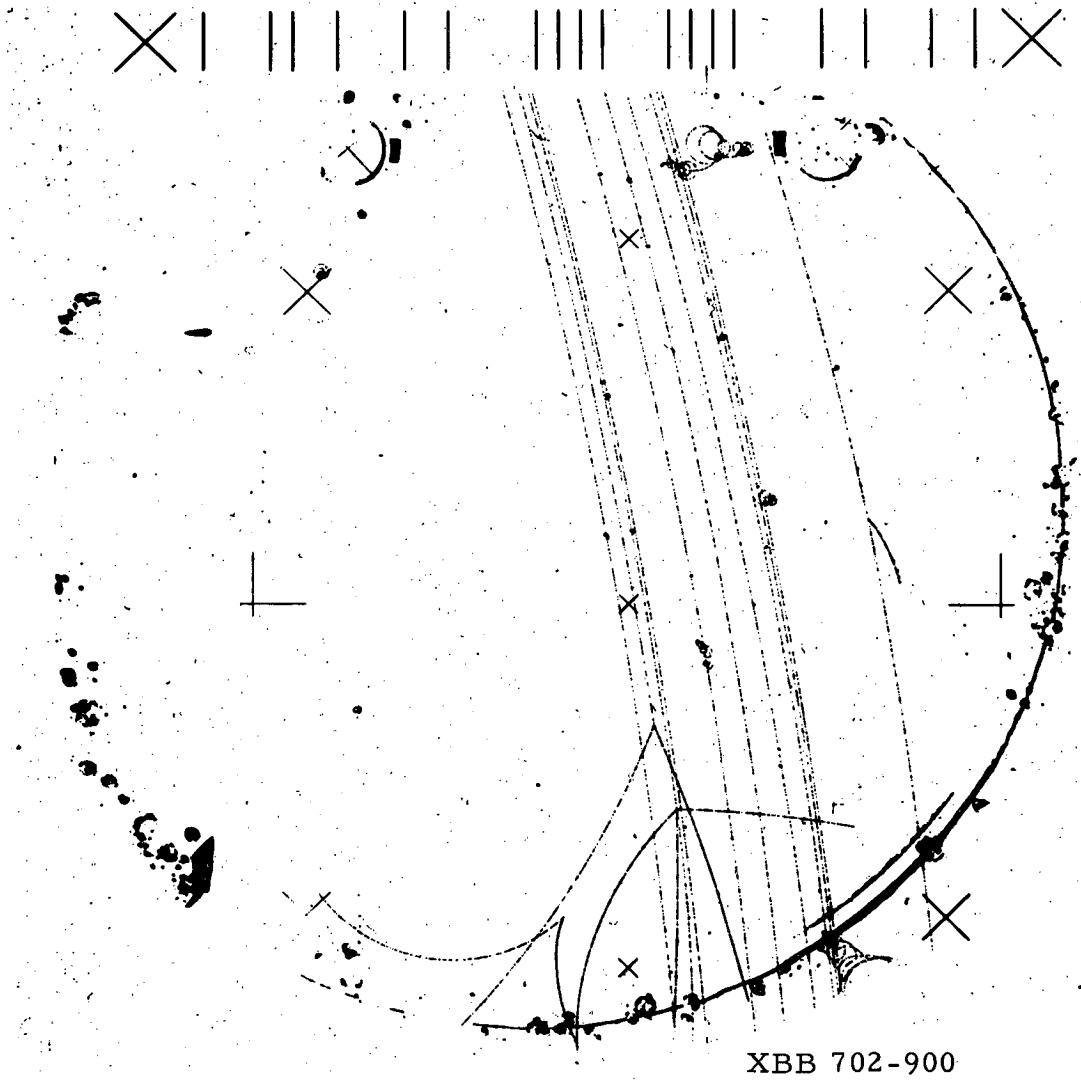
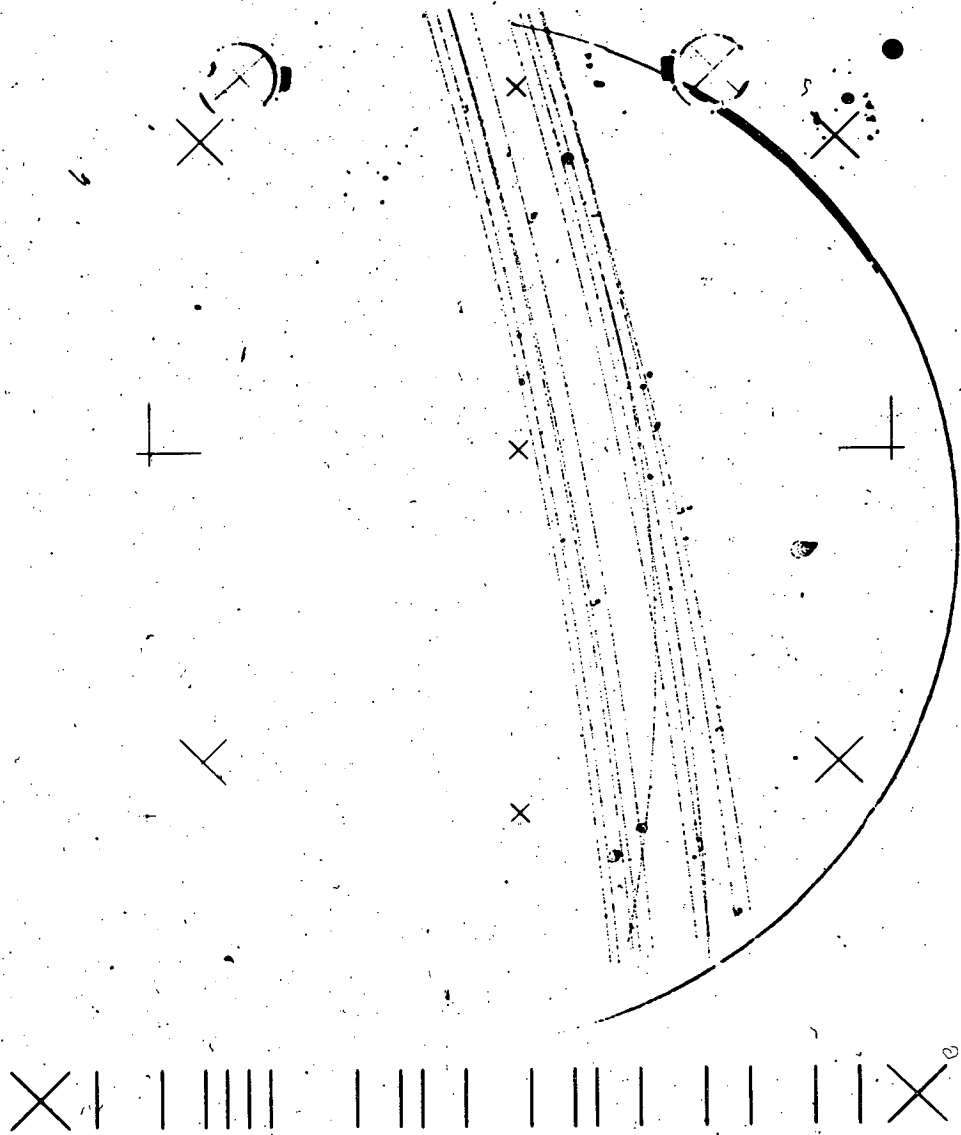


Fig. 7

XBB 702-900



XBB 702-902

Fig. 8

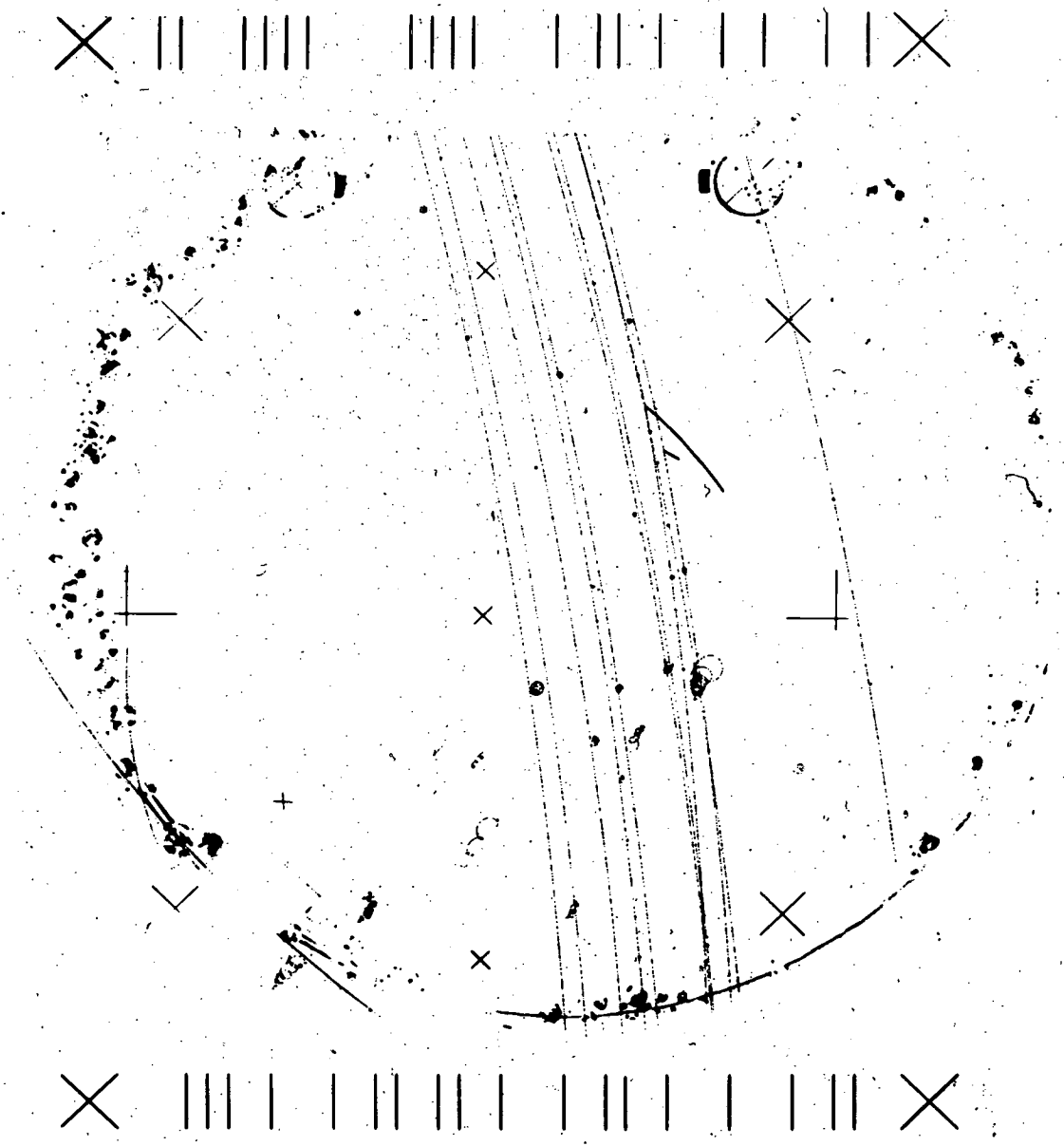
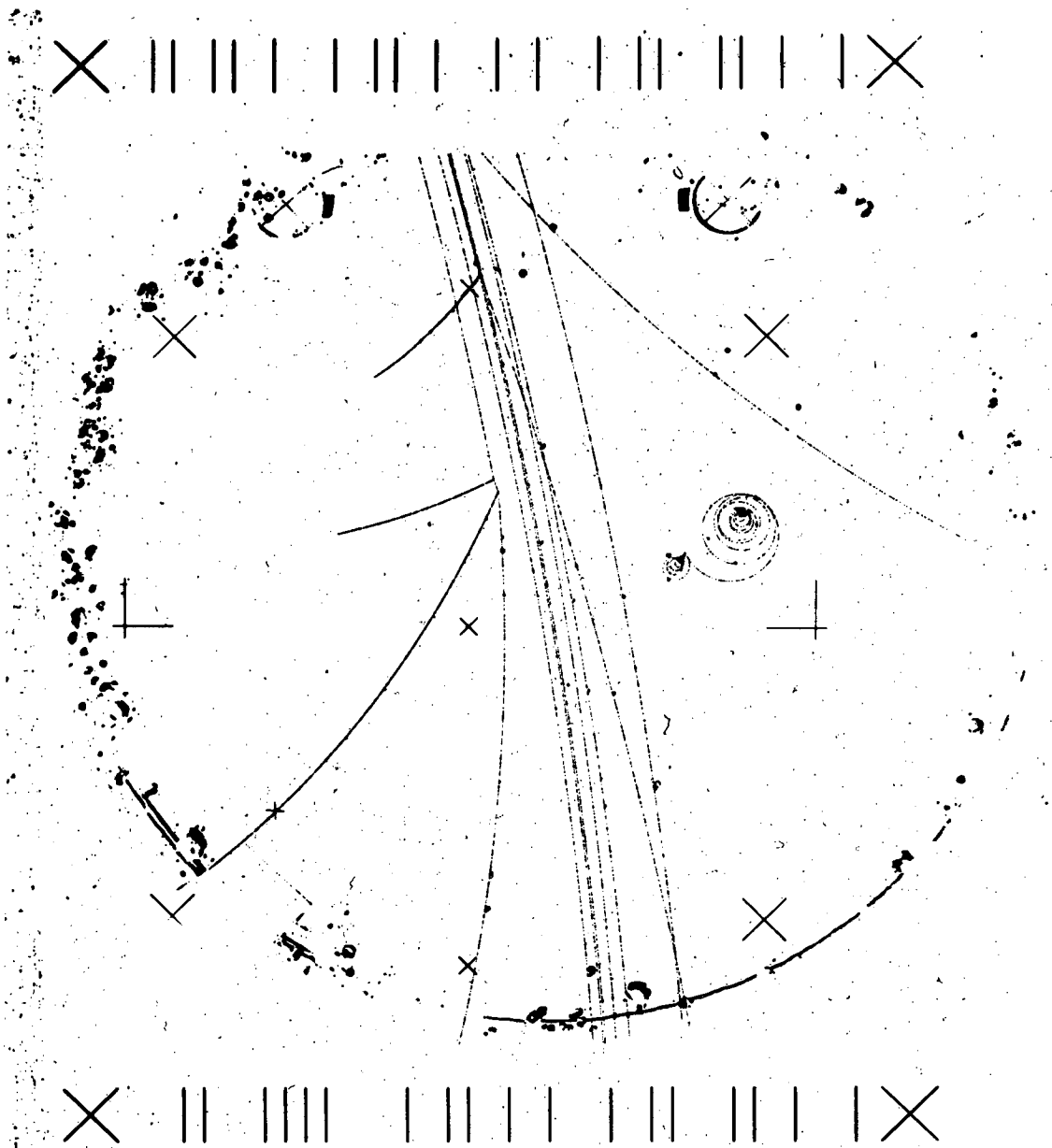


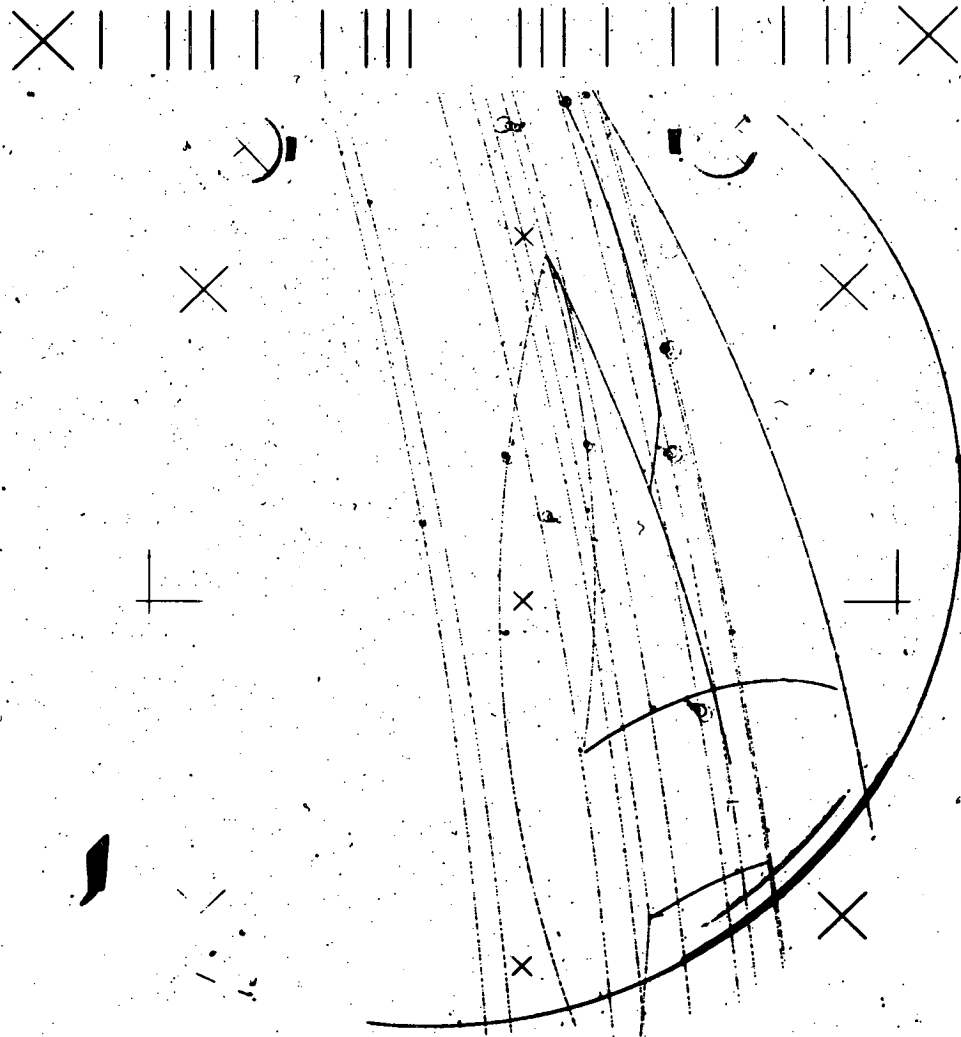
Fig. 9

XBB 702-913



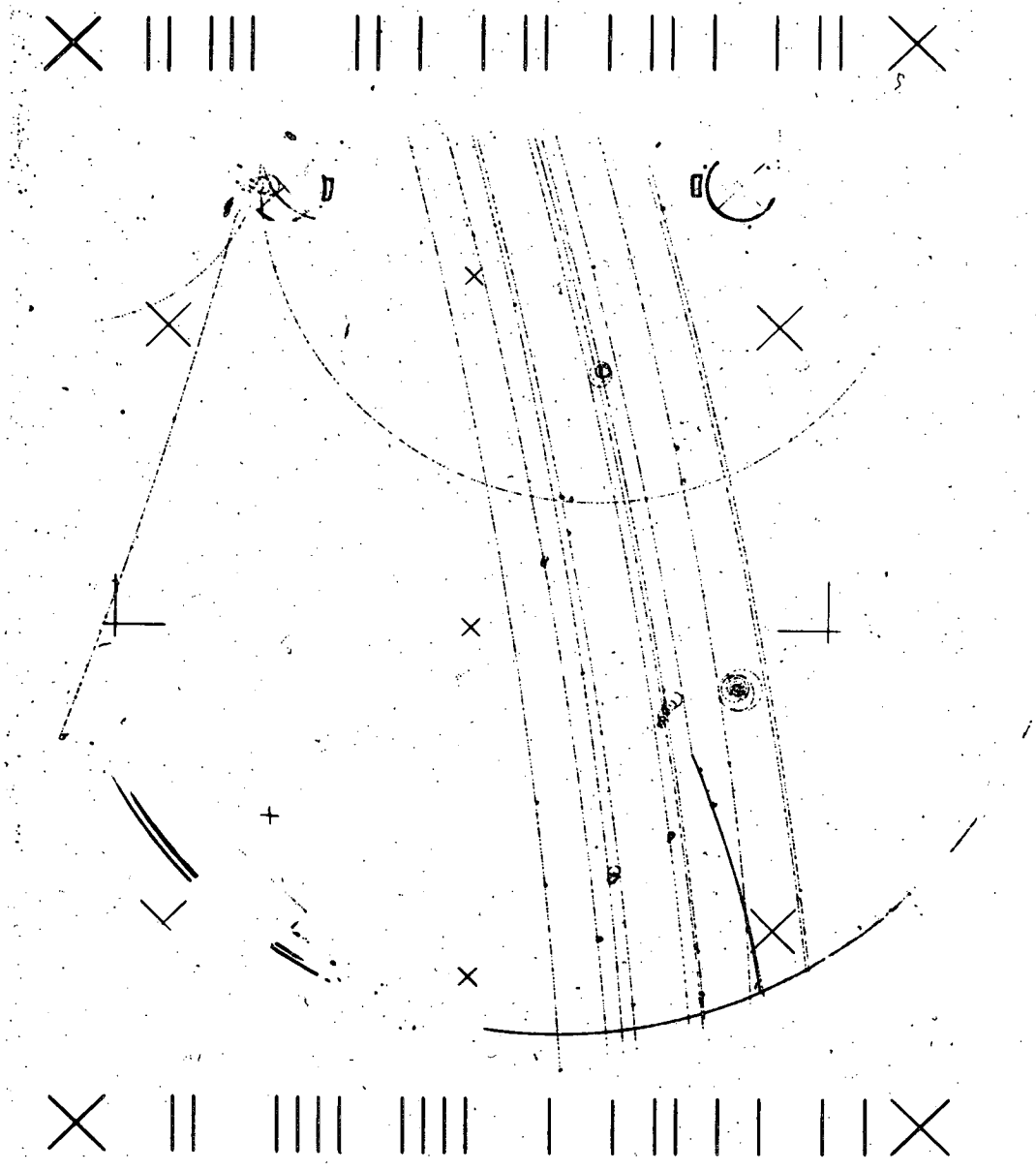
XBB 702-910

Fig. 10



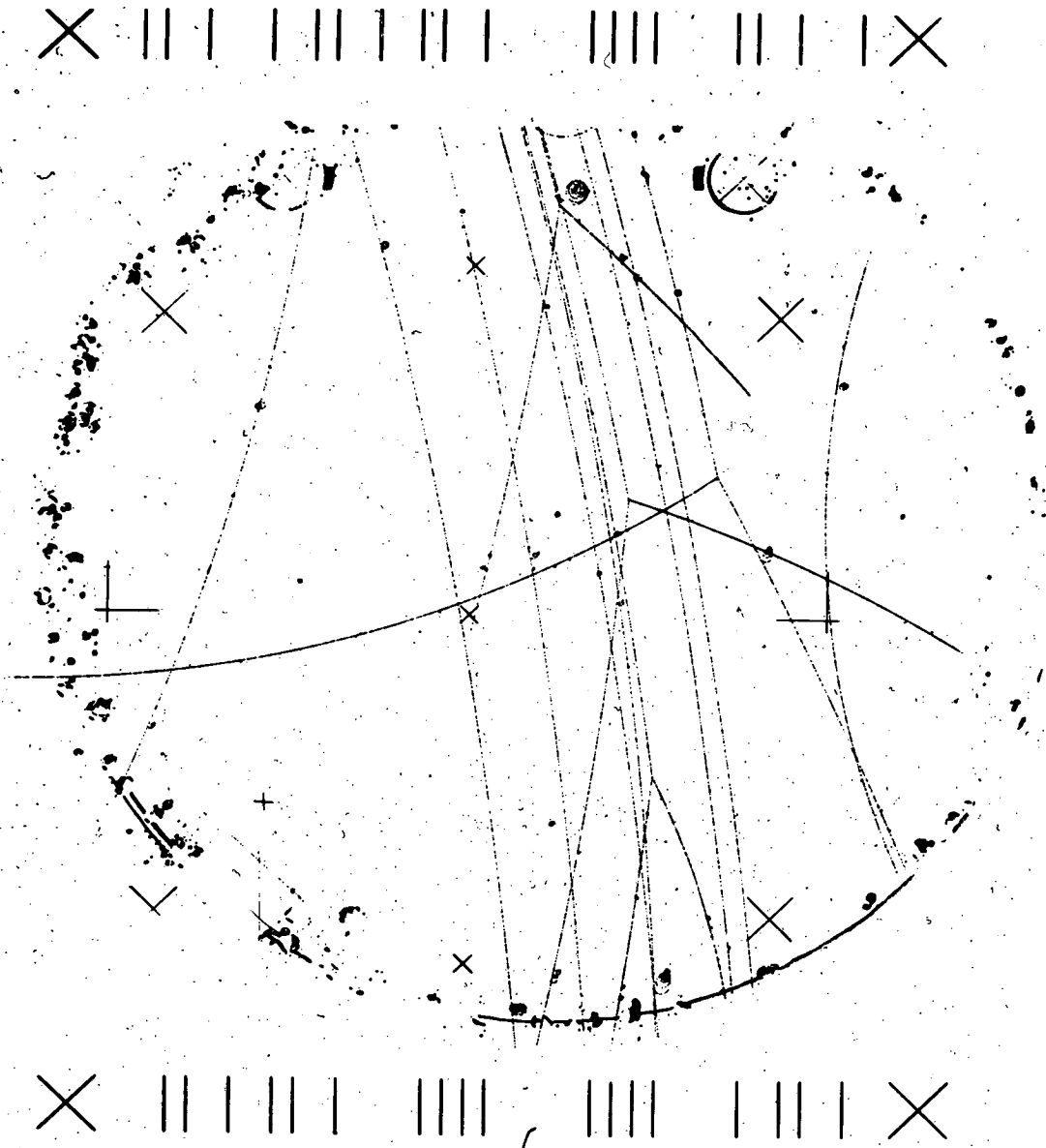
XBB 702-903

Fig. 11



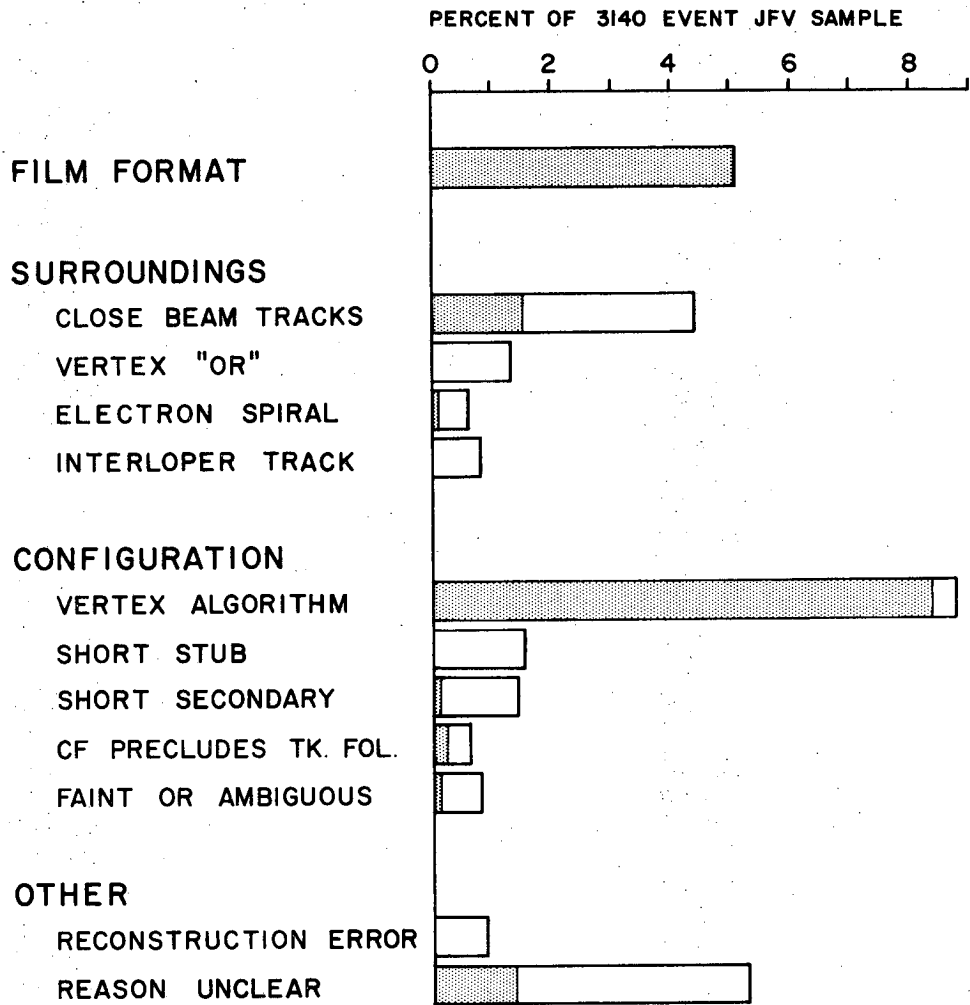
XBB 702-905

Fig. 12



XBB 702-901

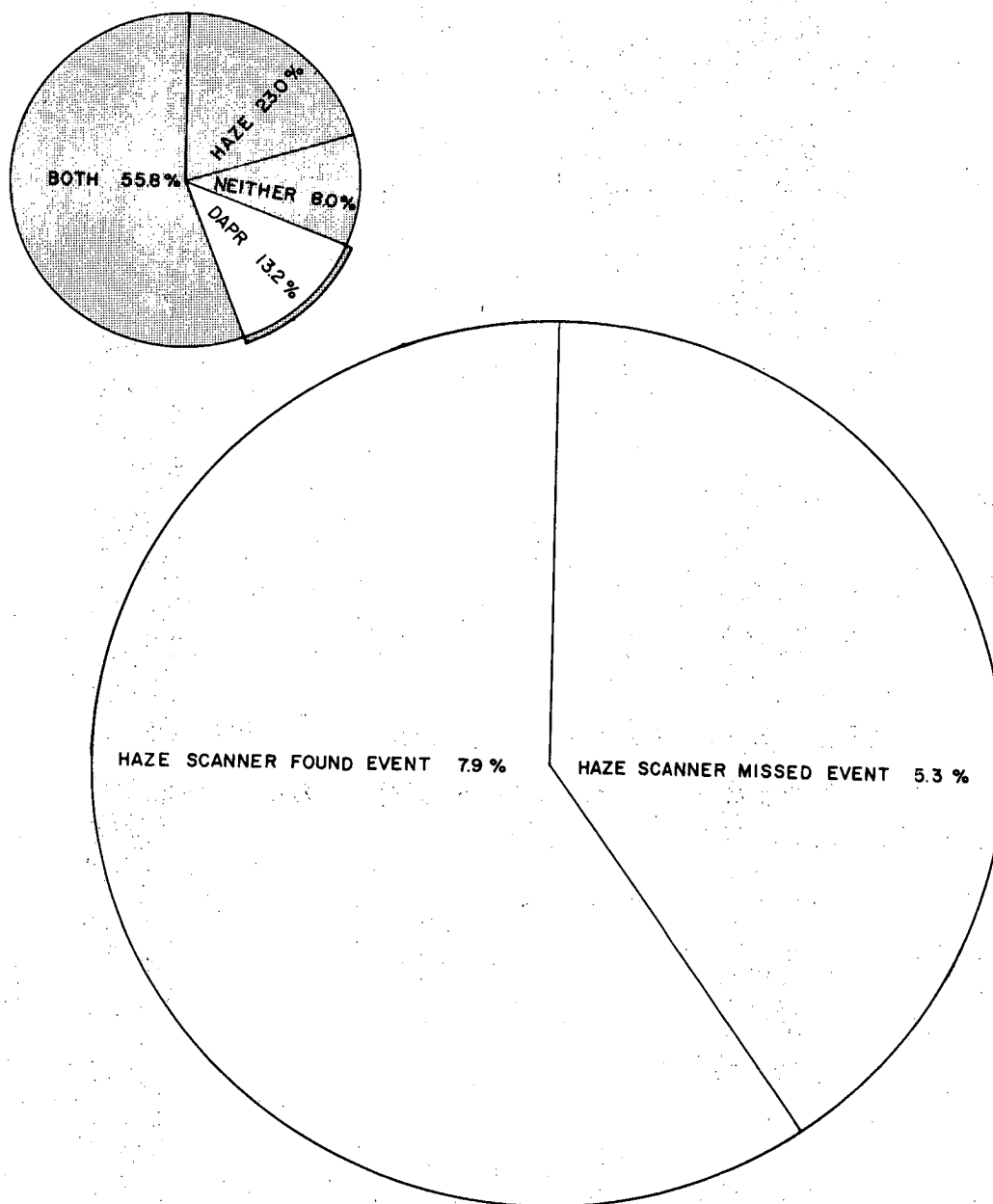
Fig. 13



DISTRIBUTION OF 974 EVENTS NOT OUTPUT BY DAPR
UNDETECTED VERTICIES SHADED

XBL 703-506

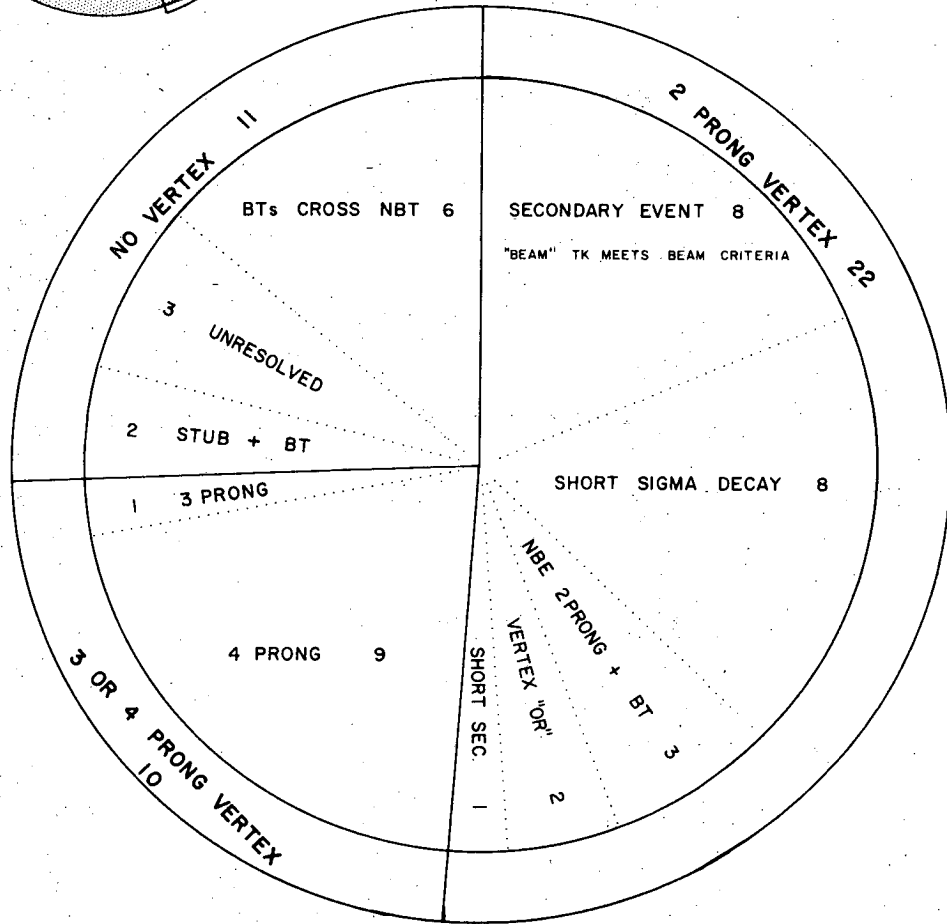
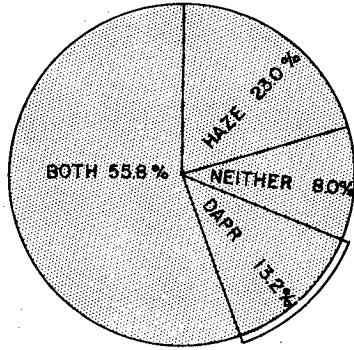
Fig. 14



DISTRIBUTION OF 414 TWO-PRONG EVENTS
DAPR ONLY (13.2% OF 3140 JFV SAMPLE)

XBL 702-403

Fig. 15



DISTRIBUTION OF 43 FAKE TWO-PRONG EVENTS
FOUND BY DAPR IN JFV OF 13,005 FRAMES SCANNED

XBL 702-405

Fig. 16

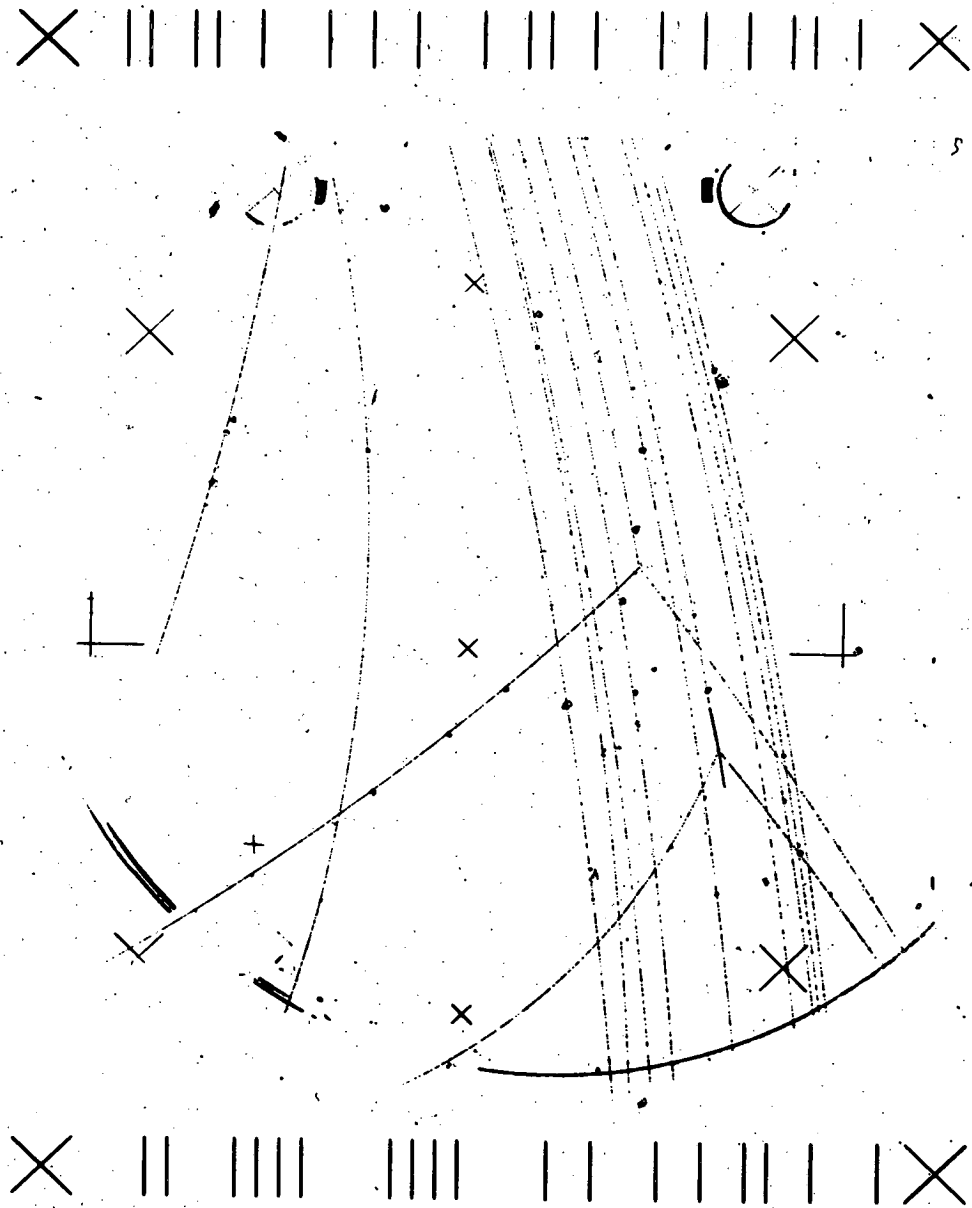
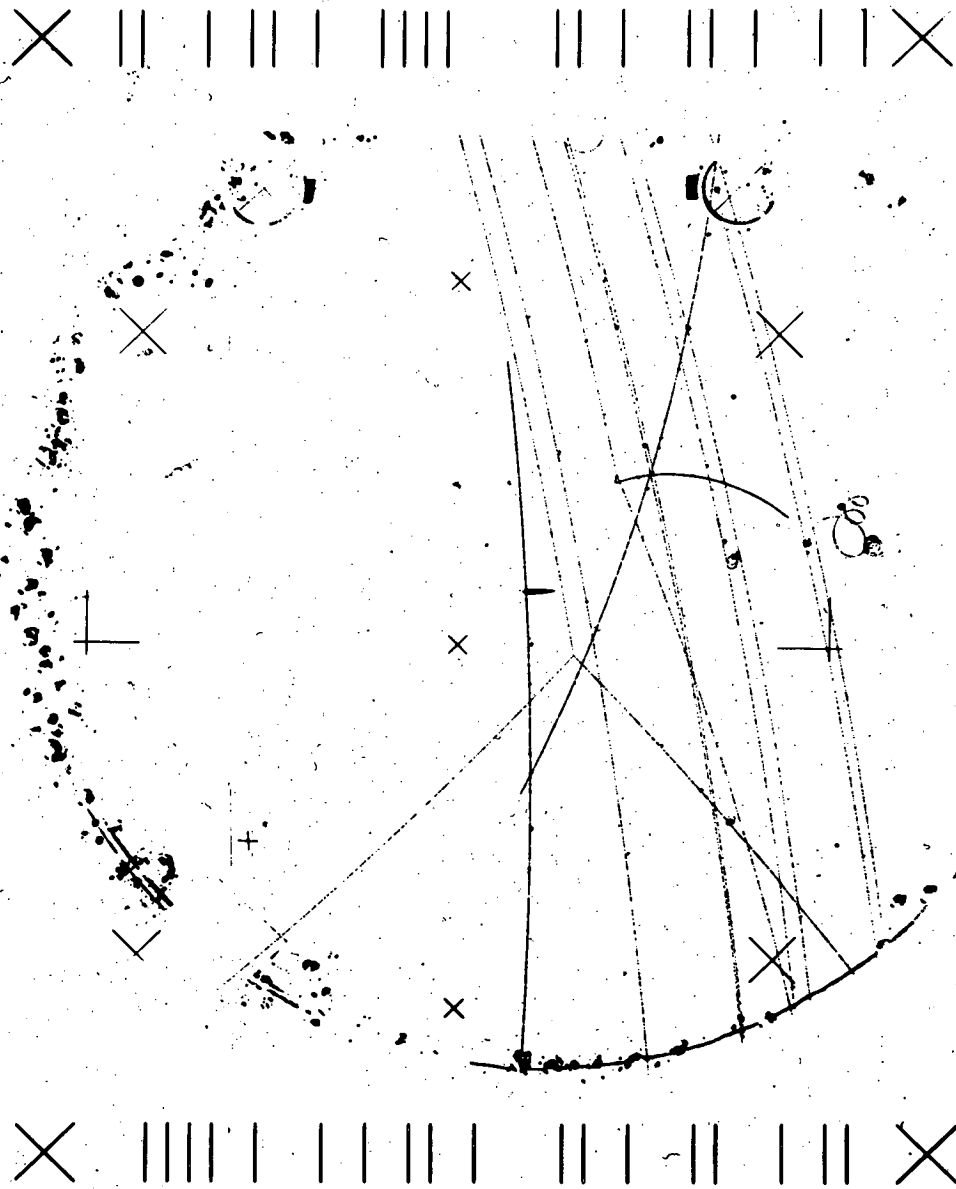


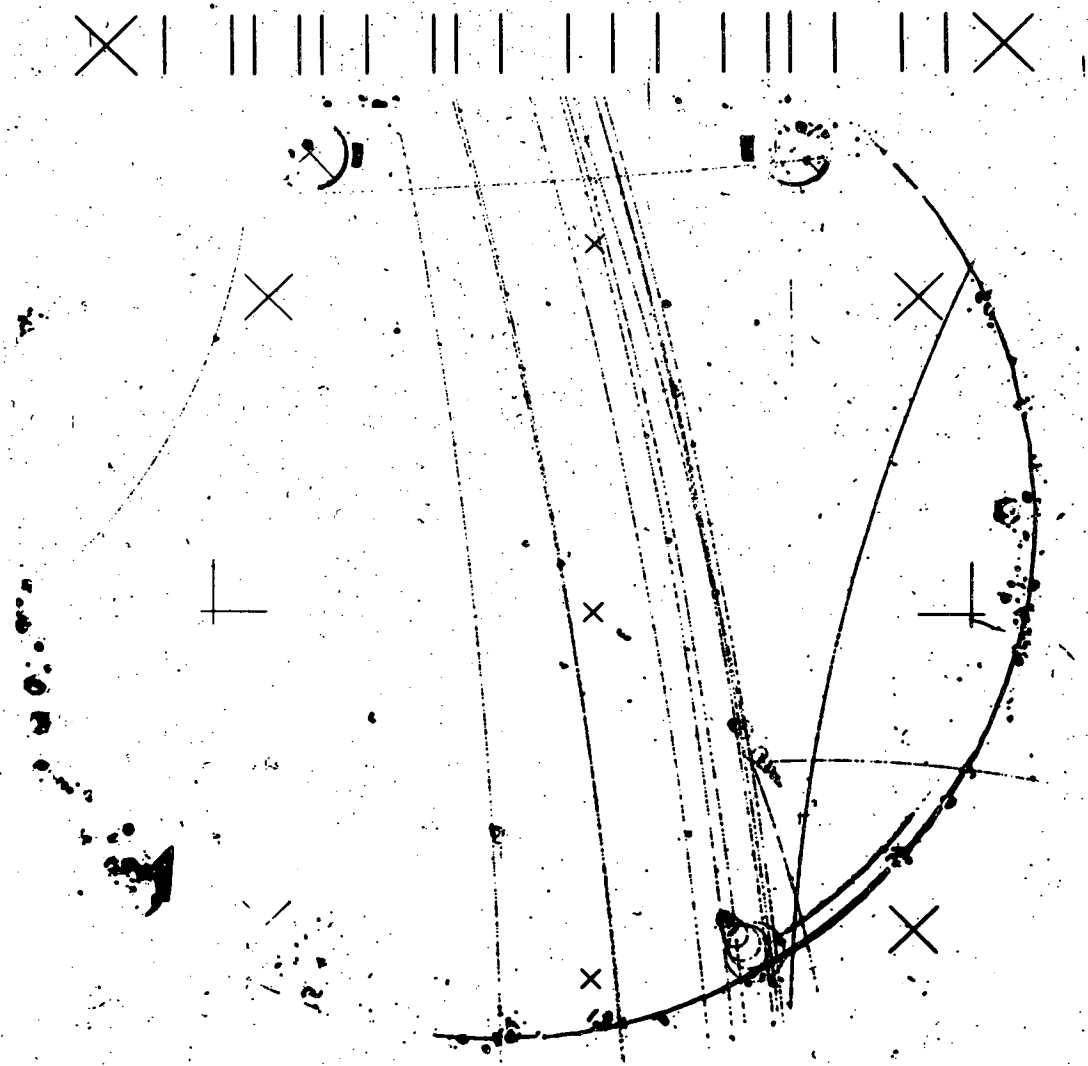
Fig. 17

XBB 702-912



XBB 702-906

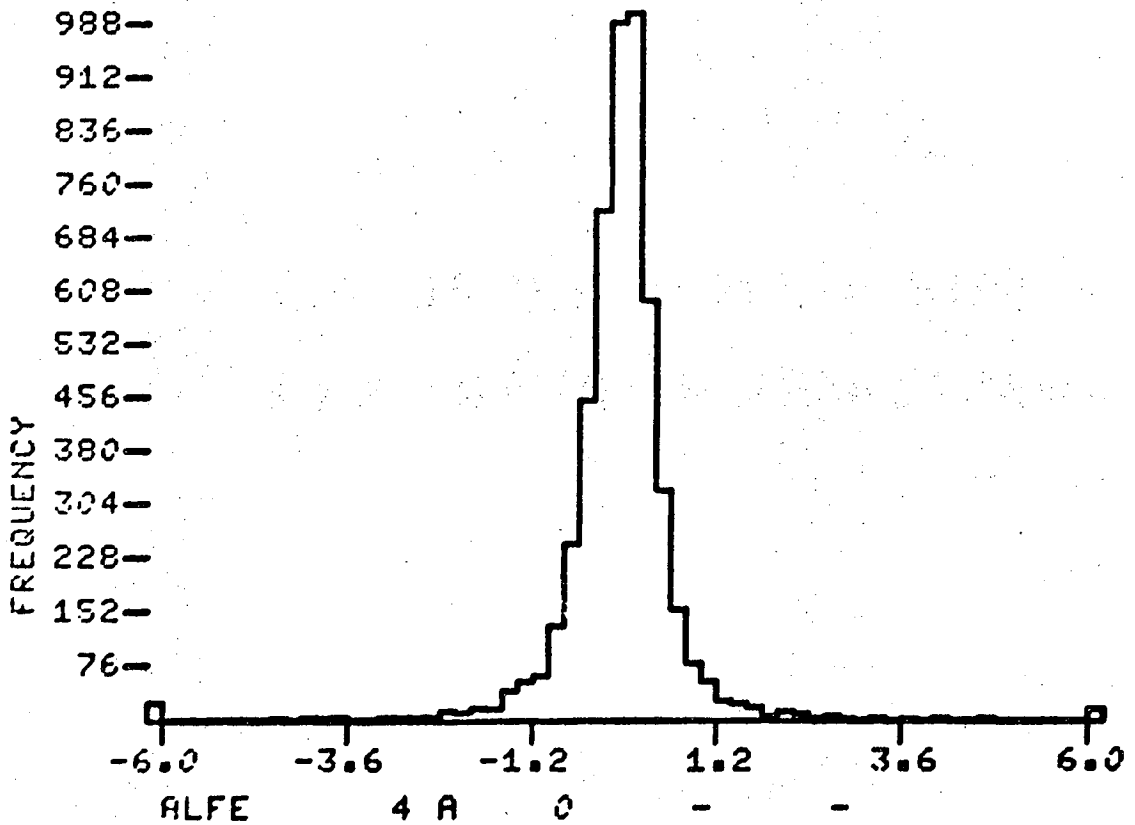
Fig. 18



XBB 702-908

Fig. 19

25 INCH HYDROGEN CHAMBER FAIR OUTPUT
RUN 053593 DATE 700219 ASN.GP AA03
LEVEL G4 HIST NO 12
U60 CELLS .2 5241 POINTS

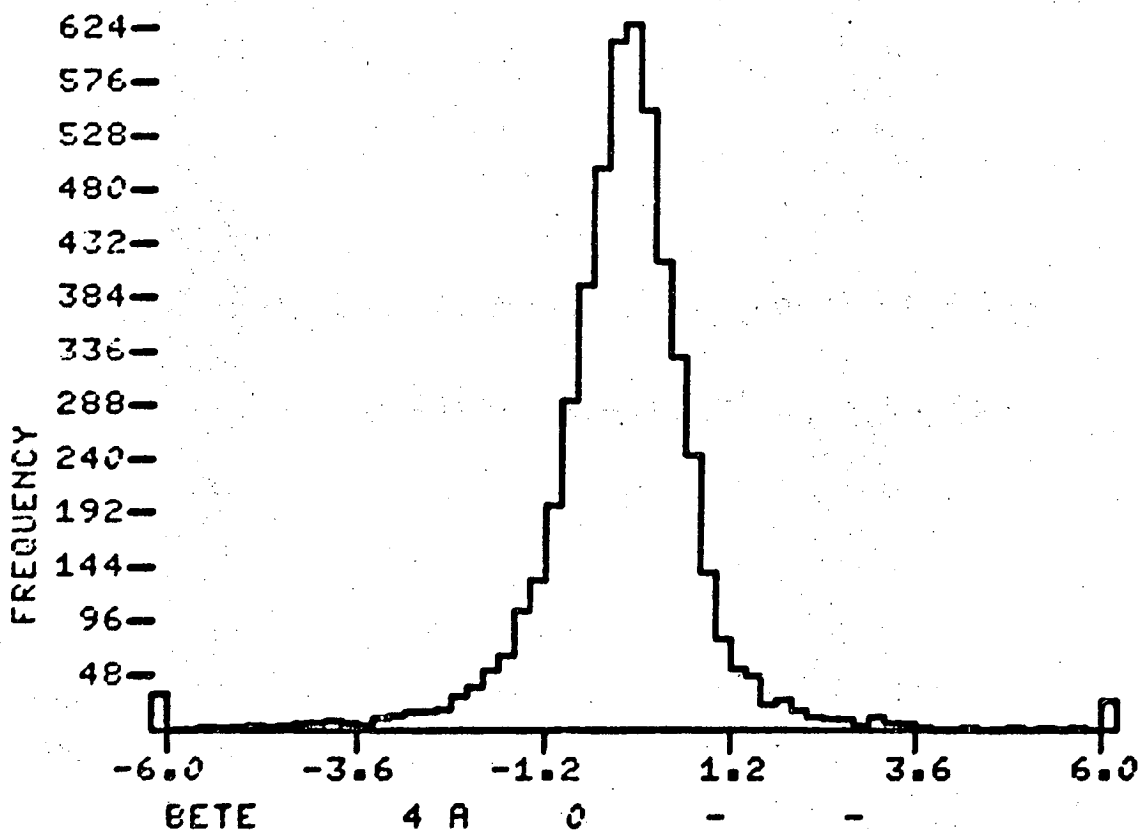


**DIP ANGLE COMPARISON
HAZE-DAPR (NORMALIZED)**

XBL 702-387

Fig. 20

25 INCH HYDROGEN CHAMBER FAIR OUTPUT
RUN 053593 DATE 700219 ASN.GP AA03
LEVEL G4 HIST NO 8
U60 CELLS .2 5241 POINTS

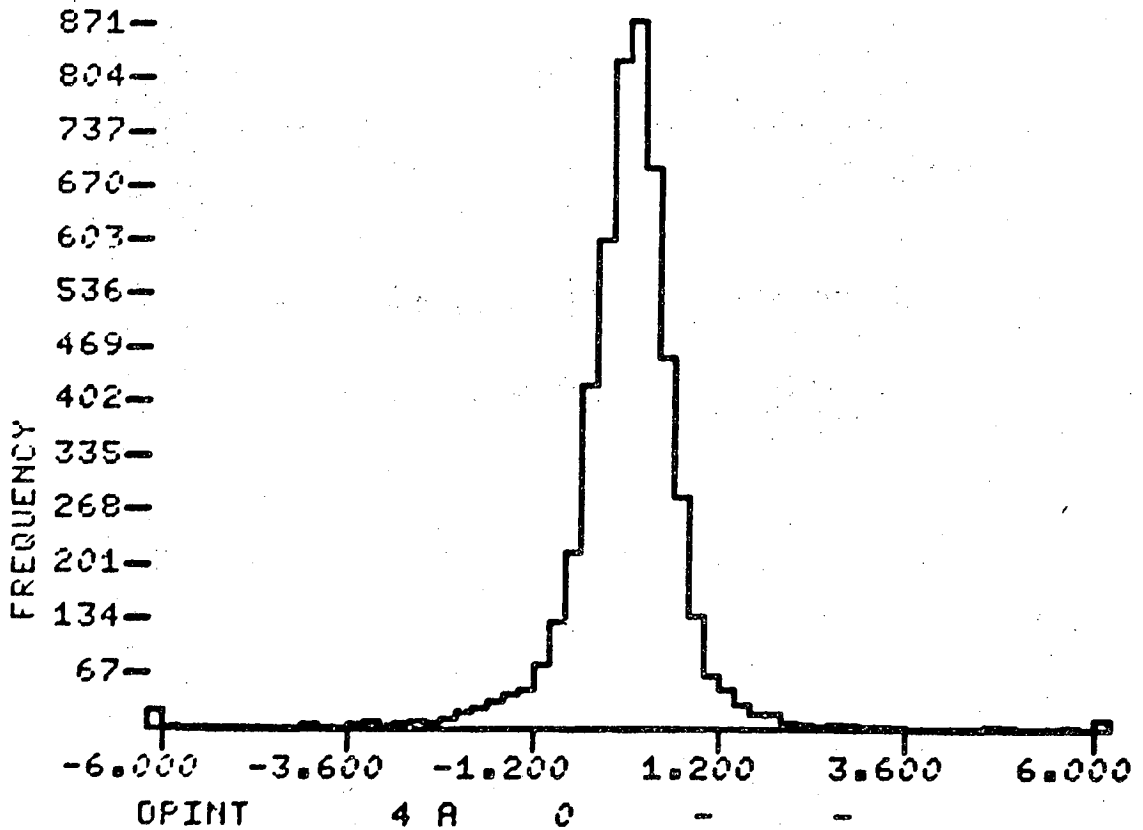


**AZIMUTH ANGLE COMPARISON
HAZE-DAPR (NORMALIZED)**

XBL 702-388

Fig. 21

25 INCH HYDROGEN CHAMBER FAIR OUTPUT
RUN 053593 DATE 700219 ASN.GP AAC3
LEVEL G4 HIST NO 4
U60 CELLS .200 5241 POINTS

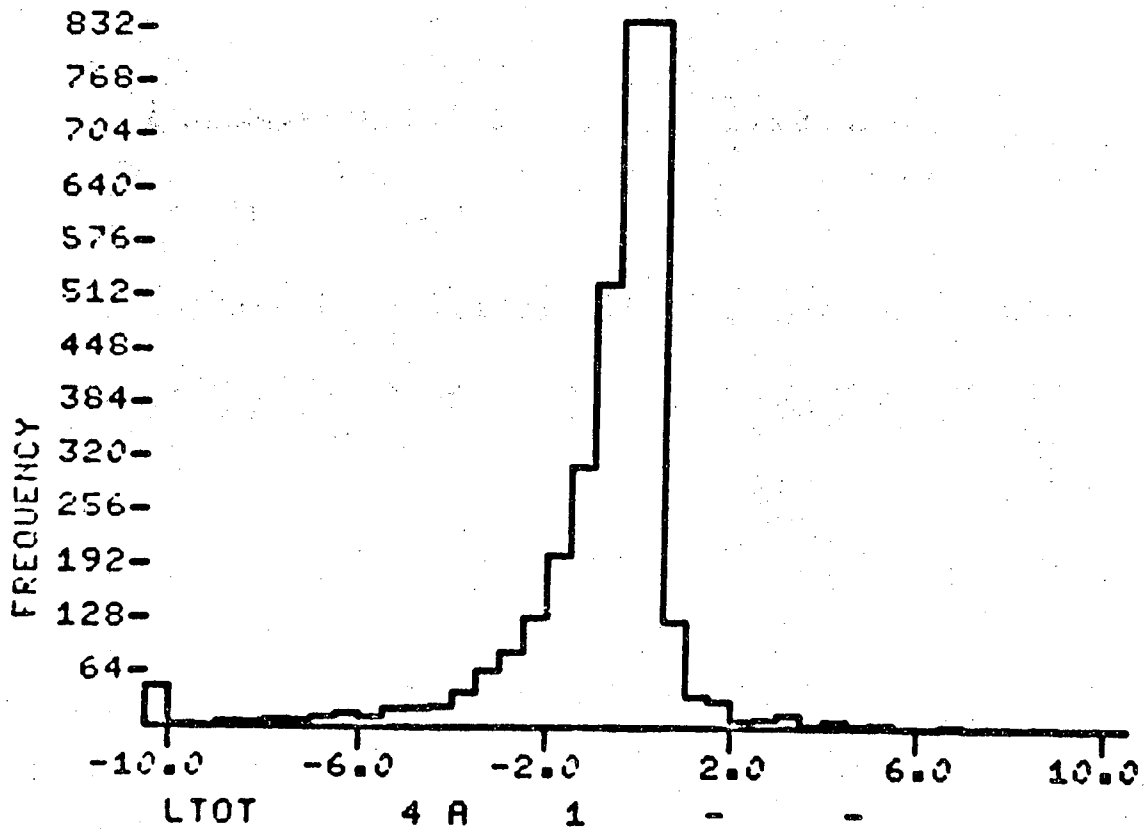


**MOMENTUM COMPARISON
HAZE-DAPR (NORMALIZED)**

XBL 702-389

Fig. 22

25 INCH HYDROGEN CHAMBER FAIR OUTPUT
RUN 053593 DATE 700219 ASN.GP AAC3
LEVEL G4 HIST NO 1
U40 CELLS .5 3494 POINTS

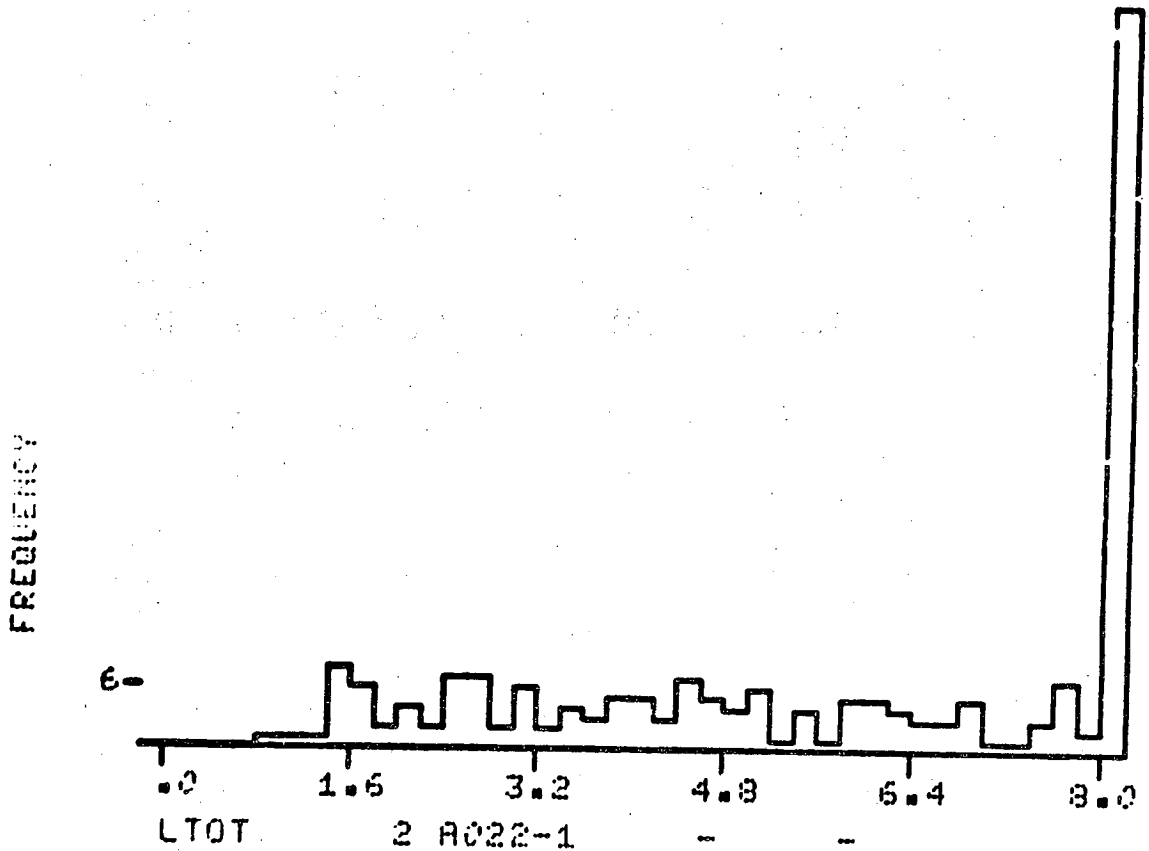


TRACK LENGTH COMPARISON HAZE-DAPR (CENTIMETERS)

XBL 702-390

Fig. 23

25 INCH HYDROGEN CHAMBER FAIR OUTPUT
RUN 049715 DATE 700130 ASN GP AA03
LEVEL A0F2E1 HIST NO 9
N40 CELLS .2 956 POINTS
LTOT FOR DAPR ELAST

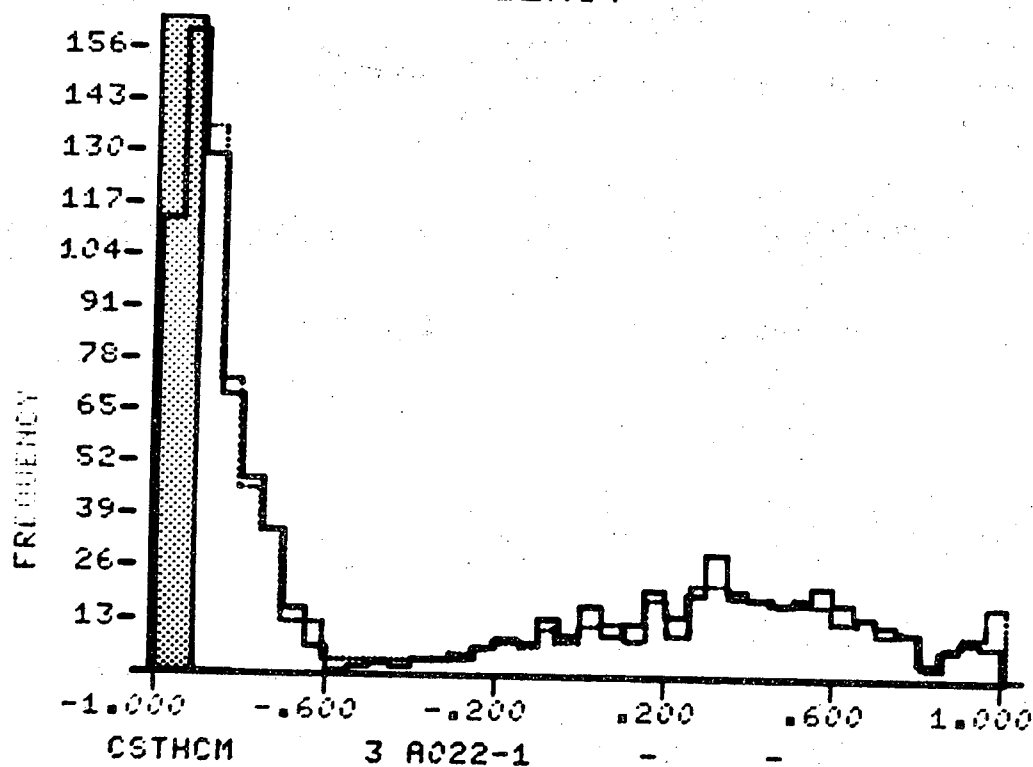


**LENGTH OF PROTON TRACK
FOR ELASTIC EVENTS (DAPR)**

XBL 702-395

Fig. 24

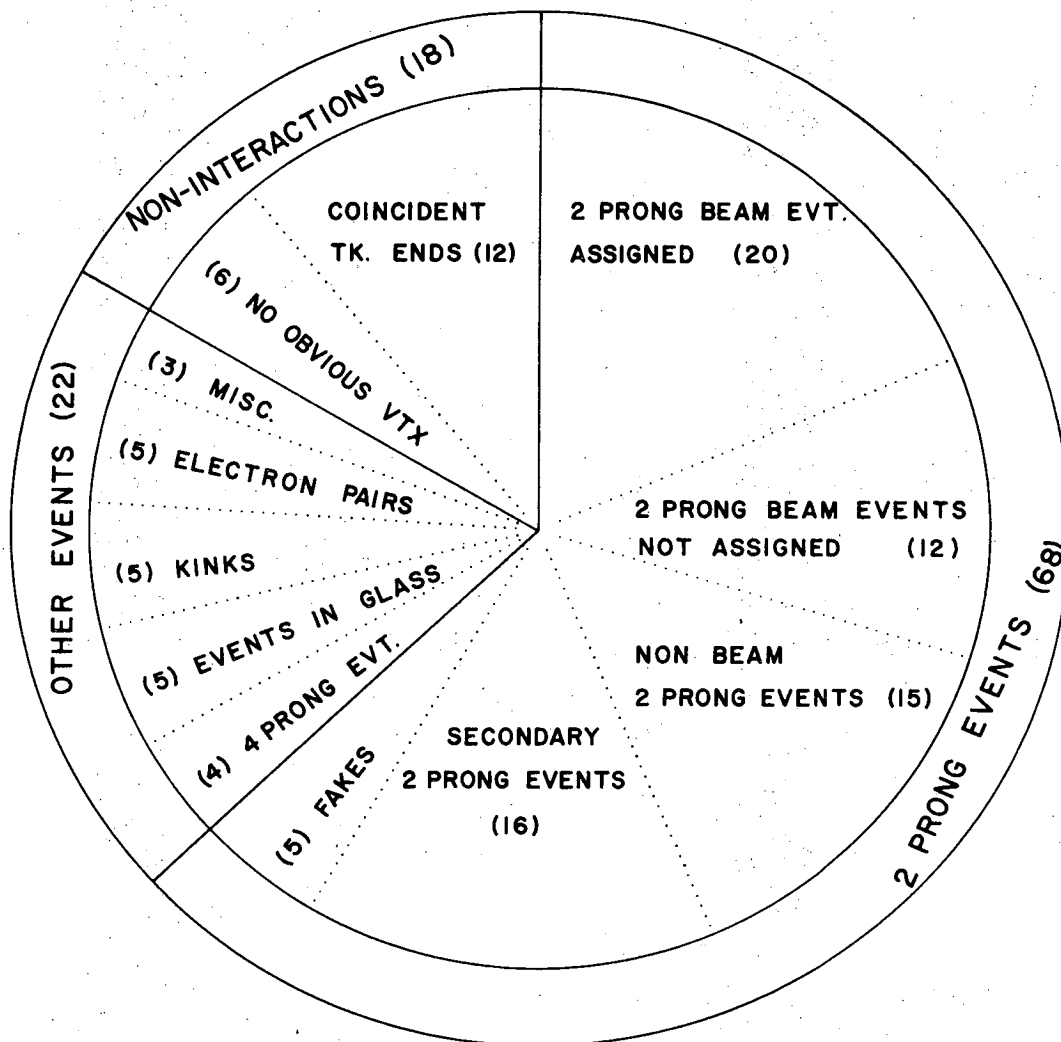
25 INCH HYDROGEN CHAMBER FAIR OUTPUT
RUN 049113 DATE 700128 ASN.GP AA03
LEVEL A0F2E1 HIST NO 1
U40 CELLS .050 954 POINTS
CSTHOM FOR DAPR ELAST



COMPARISON OF $\cos \theta^*$ DISTRIBUTIONS
..... HAZE — DAPR

XBL 702-396

Fig. 25



DISTRIBUTION OF 108 VERTICIES
FOUND BY DAPR BUT NOT HAZE SCAN
ROLL 6160 JOINT FIDUCIAL VOL

XBL 703-507

Fig. 26

LEGAL NOTICE

This report was prepared as an account of Government sponsored work. Neither the United States, nor the Commission, nor any person acting on behalf of the Commission:

- A. Makes any warranty or representation, expressed or implied, with respect to the accuracy, completeness, or usefulness of the information contained in this report, or that the use of any information, apparatus, method, or process disclosed in this report may not infringe privately owned rights; or*
- B. Assumes any liabilities with respect to the use of, or for damages resulting from the use of any information, apparatus, method, or process disclosed in this report.*

As used in the above, "person acting on behalf of the Commission" includes any employee or contractor of the Commission, or employee of such contractor, to the extent that such employee or contractor of the Commission, or employee of such contractor prepares, disseminates, or provides access to, any information pursuant to his employment or contract with the Commission, or his employment with such contractor.

TECHNICAL INFORMATION DIVISION
LAWRENCE RADIATION LABORATORY
UNIVERSITY OF CALIFORNIA
BERKELEY, CALIFORNIA 94720